The Fundamental Cycle: A Harmonic Reinterpretation of Relativity and Its Cosmological Implications

Xavi Aupí

Institut Illa de Rodes, Ctra. de les Arenes, 57, Roses, 17480, Catalonia, Spain.

Corresponding author(s). E-mail(s): xaviaupi@gmail.com;

Abstract

In this paper, we present a harmonic reinterpretation of the theory of relativity, wherein the circle emerges as the mathematical entity underlying physical reality. This approach stems from a reconsideration of the Minkowskian rotation. Its imaginary character–both in angle and in time–is attributed to the observer's embeddedness within the physical structure of reality, while the rotation itself is understood as a physical manifestation of an underlying fundamental cycle. This cycle, which operates across all physical scales, is posited as a potential organizing principle of nature, possibly reflecting a deeper layer of physical law. At its largest possible scale, this reinterpretation yields a cyclic, observer-dependent cosmological model in which the observable universe is understood as only half of a broader, more complete cosmological scheme, the other half remaining beyond direct observation. This novel perspective arises from a philosophical analysis of what is known in cosmology as the problem of the beginning, offering a logically grounded framework for the origin of the universe.

Keywords: Minkowskian rotation, cyclic cosmology

1 Introduction

In 1905, the special theory of relativity introduced a series of phenomena that were far beyond the reach of our daily experience of reality: time ceased to have its absolute connotation, becoming relative to the observer, and so did length measurements. As a consequence, we entered a domain where physical intuition lost prominence in

favor of mathematical reasoning. In this regard, the work by Minkowski in 1908 [1] represented a crucial milestone, as it identified the proper mathematical structure underlying relativity: a transformation formally equivalent to a rotation, but involving complex coordinates. Explicitly, the transformation reads:

$$x' = x\cos i\theta + iy\sin i\theta$$
$$iy' = -x\sin i\theta + iy\cos i\theta$$

where the y-coordinate relates to time according to $y = ct$ [2]. At the time, no physical explanation was offered regarding the presence of the imaginary unit; rather it was understood as a convenient mathematical device that correctly captured the physics. Following this path, most authors embraced a more abstract formulation. In particular, the relationship between the trigonometric functions of an imaginary angle and the hyperbolic functions, $\sinh\theta$ and $\cosh\theta$, led to the hyperbolic formulation of special relativity (see [3] and references therein), which today underpins the symmetry principles of quantum field theory (QFT) by governing how fields transform under Lorentz boosts and ensuring the relativistic invariance of physical laws [4, 5].

However, rather than remaining within the hyperbolic framework, here we focus on the fact that the underlying structure is fundamentally a rotation, directly connected to the geometry of the circle. The fact that it is the circle—and not any other complex curve—underlying relativity suggests a hidden simplicity that calls for a physical explanation. The aim of this article is precisely to address why the circle appears, and what role the imaginary unit plays. In particular, we will show that Minkowski's imaginary rotation results from combining two ideas: the concept of cyclicity, and the inclusion of the observer within the physical system. The former brings about the rotation, while the latter forces both the time coordinate and the angle to acquire a pure imaginary character.

Cyclic behavior is evident across a broad range of physical phenomena—from astronomical motions to atomic oscillations. Thus, the emergence of circular or rotational structures at a fundamental level is intuitively appealing and conceptually welcome. In contrast, the introduction of imaginary time, although mathematically effective, remains far less intuitive and poses deeper interpretative challenges. Whether it has a true physical basis or is merely a mathematical artifact has been considered at different stages throughout the development of theoretical physics [6–18]. Of special relevance is the work by Wick (1954) [19] who introduced the so-called Wick rotation to transform oscillatory path integrals into convergent ones in QFT, primarily as a computational tool, but its meaning has often remained abstract.

Finding a physical interpretation for the Minkowski rotation is far from being a merely academic pursuit; it carries profound implications for our understanding of reality at its most fundamental level. As outlined in this work, it enables a harmonic reinterpretation of relativity—one that naturally integrates special relativity and gravity—whose simplicity suggests a more intrinsic formulation of the theory, while also giving rise to new relativistic expressions. Furthermore, this approach yields valuable insights into the nature of spacetime and quantum gravity. Notably, two concepts

slightly emerge that may prove crucial for the future development of a unifying theoretical framework: first, that large spacetime curvatures may not be exclusive to extremely massive bodies—or other energy forms—; and second, that the dynamic structure of spacetime might be described as a superposition of harmonic oscillators of inherently complex nature. When extended to the largest cosmological scales, this harmonic interpretation offers a novel framework for understanding fundamental phenomena such as accelerated expansion, dark matter, dark energy, and even the Big Bang itself, while simultaneously lending substantial support to cosmological models based on cyclic evolution [20–22]. In light of these considerations, the physical interpretation of Minkowski rotation may serve as a fruitful starting point for further exploration, potentially contributing to a more integrated understanding of the laws governing both the microscopic and macroscopic domains.

The approach taken begins by questioning the notion of a universe with a beginning: indeed, a universe that begins spontaneously invokes the concept of spontaneous generation, which is philosophically and physically problematic. To avoid this, a conservation principle must be introduced to govern the transformation of a pre–Big Bang "substance" into the observable universe. However, to also prevent the spontaneous emergence of this primordial substance itself, the existence of a cycle between the two states must be postulated. This leads to the proposal of two distinct and opposing natures—denoted X and Y—which alternate in an eternal cycle. If X represents the *presence* of the physical universe, then Y corresponds to its *absence*. This recurring process is referred to as *the fundamental cycle*.

2 The Fundamental Cycle

The conception of the Big Bang as the beginning of time inherently entails a philosophical and physical difficulty often referred to as the problem of the beginning: how can presence arise suddenly from absolute nothingness?

If we are to take seriously the task of understanding the origin and nature of the universe, we must reject the idea that something can emerge from nothing, for such a notion undermines the very foundation of rational inquiry. This rejection is implicitly encoded in the principle of conservation—most notably, energy conservation—which asserts that entities are not created ex nihilo, but rather transformed from one state to another.

If spontaneous generation is to be avoided, it follows that a more fundamental conservation principle—broader than that of energy—must be invoked. Consequently, we are led to posit that prior to the Big Bang there existed some form of pre-physical reality that transformed into what we now identify as *presence*.

At this stage, we can say little about the nature of this antecedent state, except that it must be antithetical to presence—namely, *absence*. However, absence itself is unlikely to have arisen spontaneously either; it must have been preceded by its counterpart, presence. Therefore, it becomes evident that the only way to overcome the notion of spontaneous generation is to assume a cyclical dynamic between two opposing conditions. Indeed, if the structure of reality is grounded in logic, such a cyclical relationship emerges as the only coherent alternative. But does nature offer

any example in which two fundamentally opposing realities—such as presence and absence—alternate in a sustained dynamic?

Yes, it does. For instance, the moon cycle: the cycle of the moon alternates light and shadow, which are also two antagonistic natures since darkness is absence of light. Therefore, let this simple yet profound structure provide a natural metaphor to inquire how presence in the universe alternates with absence (Fig. 1); within this analogy—which should only be understood as a pedagogical resource to lead us to the desired formalism—, the new moon would be the equivalent of the Big Bang, while the full moon would stand for a universe at its fullness of presence.

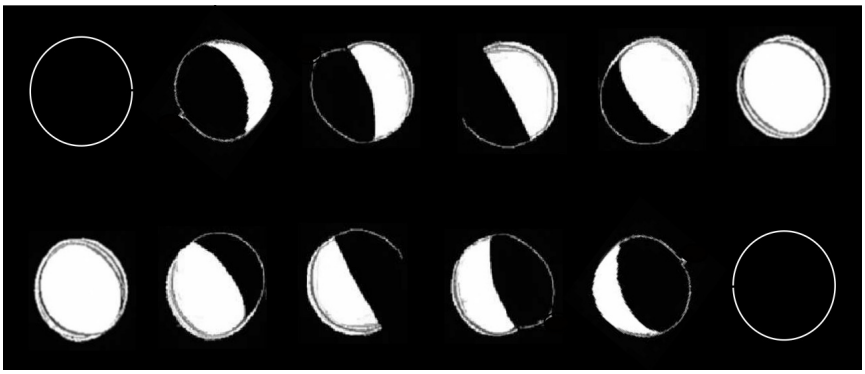

Fig. 1 Shows a symbolic representation of the phases of the moon. The moon cycle is a natural phenomenon that combines two antagonistic substances, light and darkness, just like presence and absence in the universe are assumed to be.

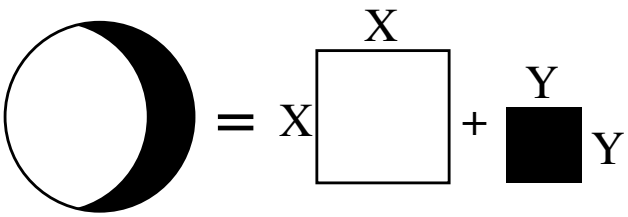

Fig. 2 Shows the illuminated and dark surface of the moon as two squares of side X and Y respectively.

Now, let us imagine that the dark region of the waning moon can be reshaped into a square of side Y, as illustrated in Fig. 2. Its area would then be Y^2. Similarly, let X^2 denote the area of the illuminated portion. The total visible surface of the moon is thus given by

$$X^2 + Y^2 = 1 \tag{1}$$

where the unit value represents the total lunar surface, expressed in suitable units. This equation is Pythagorean in nature, as it relates the legs of a right triangle. Consequently, the various phases of the moon can be graphically represented through

right triangles, as shown in Fig. 3. By superimposing these triangles, as in Fig. 4, one observes that the upper vertex of the triangle traces a circular trajectory of unit radius as the lunar phases progress. Notably, a single revolution encompasses two full moons and two new moons—indicating that the cycle is completed twice.

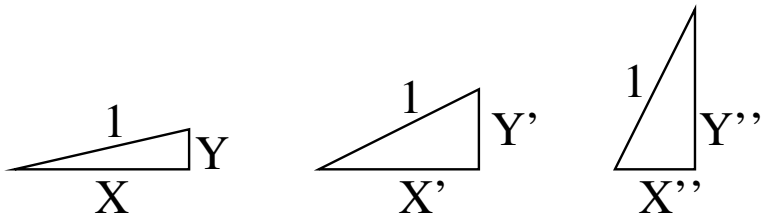

Fig. 3 Shows different right triangles corresponding to different values of lunar illumination (X) and shadow (Y). From left to right, the illuminated portion X decreases while the shadowed portion Y increases.

Assuming that the temporal evolution of the lunar phases can be described by a uniform circular motion (UCM), the angular position α at time τ can be expressed as:

$$\alpha = \omega\tau \tag{2}$$

where ω denotes the angular velocity.

2.1 Real and Imaginary

We now inquire whether an analogous expression to Eq. (1) can be established for the concepts of presence and absence in the universe.

When observing the moon, both its illuminated and dark regions are perceptible, primarily because the observer retains an external vantage point. In contrast, such equidistant observation is impossible in the case of the universe, as we are part of its very structure. Our perceptual faculties are restricted to detecting presence—analogous to the illuminated portion of the moon—while absence—corresponding to its shadow—remains entirely beyond our grasp. In this sense, absence is *inconceivable* (see Fig. 5). Nonetheless, if the analogy with the moon holds, the sum of the illuminated and shadowed areas yielding the moon's total surface should have a conceptual counterpart in the universe. In other words, our only hope for accounting for the invisible lies in the assumption that the sum of presence and absence results in a total quantity, such that absence could be inferred by subtracting presence from this total.

In the case of the moon, light and darkness are not entirely independent entities: they are defined through their mutual opposition. Darkness is the absence of light, and light the absence of darkness. If numerical values were to be assigned, one might associate light with positive real numbers and darkness with negative real numbers,

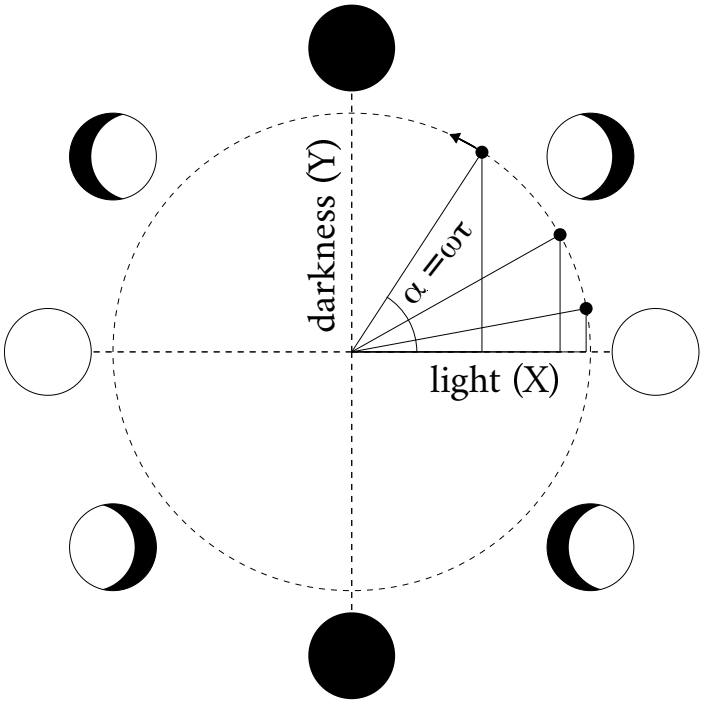

Fig. 4 Superimposed triangles from Fig. 3, arranged on coordinate axes representing light and darkness. The temporal evolution of lunar phases is modeled as a uniform circular motion, with the angle α varying linearly with time τ. Notably, a single revolution around the circle encompasses two complete lunar cycles.

whereby the sign reflects their antagonistic relation. The product

$$(-) \cdot (-) = +$$

then becomes the algebraic analogue of the proposition that the absence of darkness is light.

However, this numerical representation falls short when applied to the universe. While the use of positives and negatives may capture the antagonism between presence and absence, it fails to convey the deeper notion that absence appears inconceivable from within presence.

How, then, can this be addressed? We know that physical reality is quantified using real numbers. It follows that absence should be represented by a class of numbers that, from the standpoint of the real, appears similarly inconceivable.

Do such numbers exist? Indeed, they do: the imaginary numbers—those defined by the square root of negative one, denoted by the symbol i. From the perspective of real numbers, i is a mathematical impossibility, as no real number squared yields -1. Thus, it is fundamentally inconceivable from the standpoint of the real. At the same

time, the antagonistic relationship is preserved, since the product

$$i \cdot i = -1 \tag{3}$$

implies that the imaginary of the imaginary is real, thereby expressing the proposition that the proposition that the absence of absence is presence.

Henceforth, we adopt the following interpretative principle:

- *Presence and absence in the universe relate to one another analogously to real and imaginary numbers.*

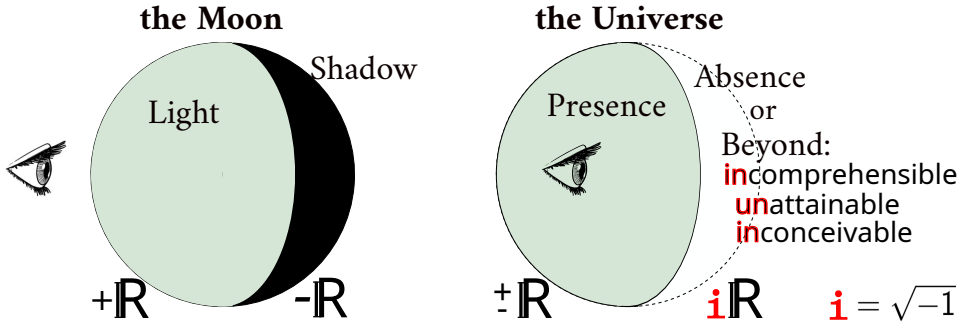

Fig. 5 Shows the essential distinction between the case of the Moon and that of the Universe. While the Moon can be observed from an external vantage point—allowing us to simultaneously perceive both its illuminated and dark regions—the Universe, by contrast, can only be experienced from within. Consequently, we only have access to what is present, whereas absence—what lies beyond—is fundamentally inaccessible, incomprehensible, or inconceivable. If one were to assign algebraic values to the Moon's light and shadow, one might naturally use positive and negative real numbers, respectively, with the sign encoding their antagonistic relationship. In the case of the Universe, however, in addition to this antagonism between presence and absence, one must also capture the inconceivable nature of absence. This is achieved by introducing the imaginary unit.

From the above considerations, it follows that Fig. 4 must be modified to describe the universe by assigning imaginary values to the y-axis, as shown in Fig. 6.

2.2 A view from within

Note that the quantities X and Y in Fig. 6 continue to satisfy the Pythagorean relation in Eq. (1). At first glance, this may appear surprising, since converting the y-axis to imaginary seems to have had no effect on the expression. However, this invariance holds only from an external perspective: when viewed from outside the system, both X and Y are interpreted merely as geometric lengths in the plane.

Yet, if X and Y are to represent the distinct natures of presence and absence, then they cannot be treated on equal footing. Rather, they must preserve their real and imaginary identities at all times. Although they may appear equivalent from the outside—simply as coordinates in a diagram—from an internal perspective their qualitative differences must be preserved. That is:

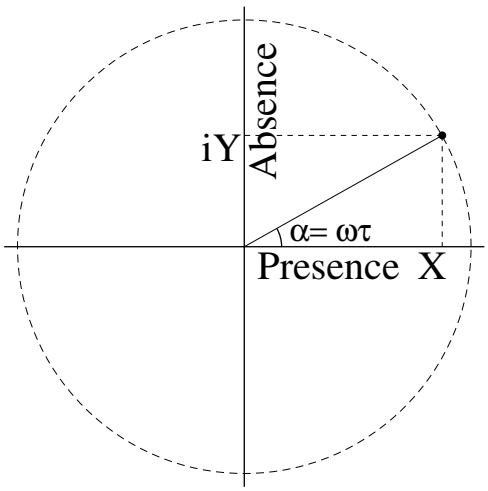

Fig. 6 Depicts a Uniform Circular Motion (UCM) representing the cyclic transition between presence and absence. This diagram adapts the lunar phase analogy to the conceptual framework of the Universe, where the imaginary axis accounts for the inaccessibility of absence.

- *If we inhabit a world that is real, then from the standpoint of being (or presence), the invisible—or absence—appears as something incomprehensible and inconceivable. Consequently, any quantities used to describe it must also reflect this inconceivability within mathematics, for example, through the use of the imaginary unit,* $\sqrt{-1}$*. Thus, what appears externally as* Y *must be represented internally as* iY*.*

This leads us to the key shift in perspective, formalised as:[1]

$$Y \quad \rightarrow \quad iY \tag{4}$$

Thus, although Fig. 6 visually designates the y-axis as imaginary, this reinterpretation must also be applied in all relevant equations, using iY instead of Y, to ensure the point of view remains internal to the structure.

For example, applying this substitution to Eq. (1) yields a reformulated expression that reflects an internal perspective:

$$X^2 + (iY)^2 = 1 \quad \Rightarrow \quad X^2 - Y^2 = 1 \tag{5}$$

In other words, while externally the system exhibits circular geometry—as captured by Eq. (1)—an internal observer perceives it as hyperbolic, consistent with Eq. (5). Hence, once one is embedded within the physical system, the geometry associated with the fundamental cycle becomes hyperbolic in nature.

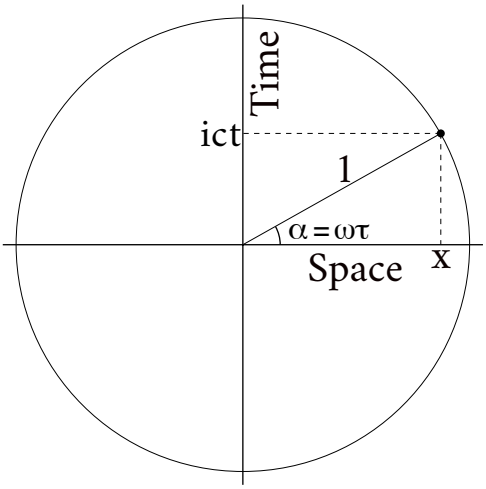

Fig. 7 The cyclic interplay between presence and absence is here associated with the two fundamental physical quantities: space x and time t. Accordingly, the transition between presence and absence manifests physically as a spacetime rotation.

2.3 Connection with physics

One may now ask: does this internal reinterpretation of circular geometry—represented by Eq. (5)—have any physical significance? To physicists, the answer is immediate: it bears a strong resemblance to the *relativistic invariant interval*:

$$x^2 - c^2t^2 = 1$$

where x denotes space, t denotes coordinate time, and c is the speed of light in vacuum. By comparing the two expressions, one can infer that what has been referred to as presence (or real) corresponds to spatial dimensions, while absence (or imaginary) maps onto time. That is,

$$X \to x \qquad Y \to ct \tag{6}$$

Let us provisionally assume the validity of this identification; the following section will investigate its consistency in more detail. Under this assumption, Fig. 6 is transformed into Fig. 7, such that the fundamental cycle of presence and absence becomes reinterpreted as a form of *spacetime rotation*.

Combining the substitutions in Eqs. (4) and (6), one obtains the transformation:

$$y \quad \to \quad ict \tag{7}$$

which may now be understood as the algebraic operation that bridges the external and internal perspectives.

Finally, note that if Eq. (6) holds, as the next section will argue, it implies that the cycle between presence and absence is not unique to the Universe as a whole. Rather,

[1] Alternatively, one might consider $Y \to -iY$, which aligns more closely with the standard Wick rotation, though at this stage such a choice is not essential.

it must manifest across all scales, consistent with the universal validity of the laws of relativity.

3 The Minkowski Rotation

We have just shown that the equation of the circle $X^2 + Y^2 = 1$ representing the fundamental cycle changes to $X^2 - Y^2 = 1$ when the observer is part of the structure. This expression was then identified as the invariant relativistic interval. To check whether this correspondence makes any sense, we now apply the same inner perspective (4) to other properties of the cycle, i.e. of the circle: in particular, the next property to consider is the rotation transformation. It will be shown that it becomes the Minkowski's rotation, thereby strengthening the validity of (6).

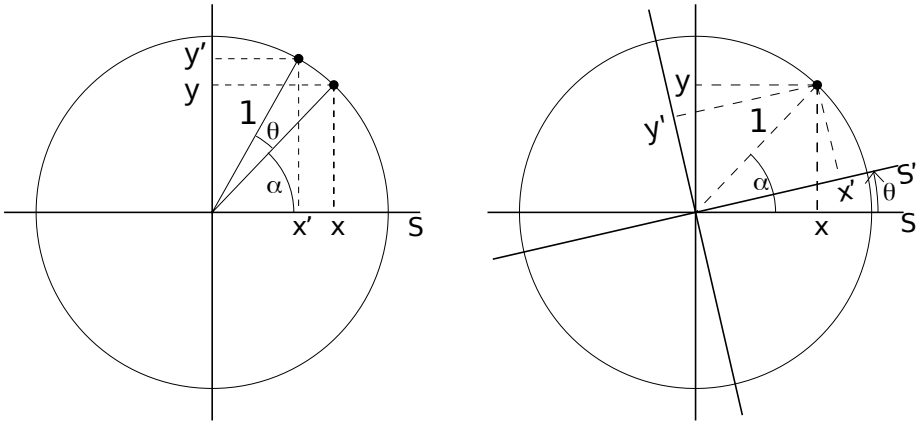

Fig. 8 Left: A point on the unit circle rotates counterclockwise an angle θ. **Right**: The S'-axes rotate θ counterclockwise.

From Fig. 8-*Left* one has

$$x = R\cos\alpha \tag{8}$$
$$y = R\sin\alpha \tag{9}$$
$$x' = R\cos(\alpha+\theta) = R\cos\alpha\cos\theta - R\sin\alpha\sin\theta \tag{10}$$
$$y' = R\sin(\alpha+\theta) = R\sin\alpha\cos\theta + R\cos\alpha\sin\theta \tag{11}$$

which become the standard transformation that rotates points in the xy-plane counterclockwise through an angle θ with respect to the x axis:

$$x' = x\cos\theta - y\sin\theta$$
$$y' = x\sin\theta + y\cos\theta$$

To rotate the axes rather than the point one should replace θ by $-\theta$ (Fig. 8-*Right*):

$$x' = x\cos\theta + y\sin\theta \tag{12}$$
$$y' = -x\sin\theta + y\cos\theta \tag{13}$$

Now, to obtain a "look from the inside" one needs to apply Eq. (4), which in this

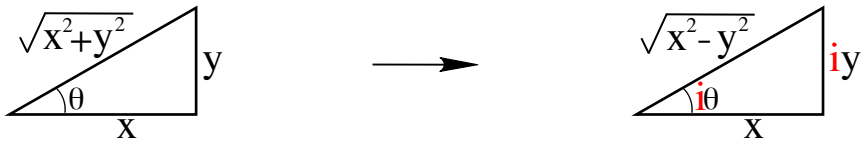

Fig. 9 Shows how the triangle used to define the sine and cosine functions changes when replacing the vertical leg y by iy. For $-\pi/4 < \theta < \pi/4$, the angle θ becomes a pure imaginary value $i\theta$.

context implies to replace all real y-values by pure imaginary values of the type iy, and not only in Eqs. (12)-(13), but also in (8)-(9) and in the sine and cosine definitions too. The latter is achieved by replacing the vertical leg y of the triangle in Fig. 9 by its imaginary counterpart iy, such that the sine and cosine now become:

$$\cos\theta = \frac{x}{\sqrt{x^2+y^2}} \quad \rightarrow \quad \frac{x}{\sqrt{x^2-y^2}} \equiv \cos z \qquad z \in \mathbb{C} \tag{14}$$
$$\sin\theta = \frac{y}{\sqrt{x^2+y^2}} \quad \rightarrow \quad \frac{iy}{\sqrt{x^2-y^2}} \equiv \sin z \qquad z \in \mathbb{C} \tag{15}$$

where the argument θ has turned into a complex number z. In particular, whenever the absolute value of x is greater than that of y, which corresponds to the domain of special relativity—for which the relative velocity v_g satisfies $v_g < c$—, the argument is a pure imaginary value, such that it can be written as $z = i\theta$. Therefore, applying $y \rightarrow iy$ within the domain $v < c$ transforms expressions (8)–(9) and (12)–(13) into

$$x = R\cos i\alpha$$
$$iy = R\sin i\alpha$$
$$x' = x\cos i\theta + iy\sin i\theta$$
$$iy' = -x\sin i\theta + iy\cos i\theta$$

Now, relating the y-values to the time coordinate according to (6) and writting $\alpha = \omega\tau$ as stated by (2), one obtains

$$x = R\cos i\omega\tau \tag{16}$$
$$ict = R\sin i\omega\tau \tag{17}$$
$$x' = x\cos i\theta + ict\sin i\theta \tag{18}$$
$$ict' = -x\sin i\theta + ict\cos i\theta \tag{19}$$

where the last two constitute the Minkowski rotation, which is formally equivalent to the Lorentz transformation. Indeed, consider the specific rotation illustrated in Fig. 10. The S' axes are rotated by an angle θ such that the original x-axis is mapped onto the position of point P. In this case, $t' = 0$ and $\theta = \alpha$. Substituting these values into Eq. (19) yields the following expression for a magnitude with velocity units:

$$\frac{c^2 t}{x} = -ic\frac{\sin i\theta}{\cos i\theta} = -ic\frac{\sin i\alpha}{\cos i\alpha} \equiv v_g \tag{20}$$

Then, applying the trigonometric identity

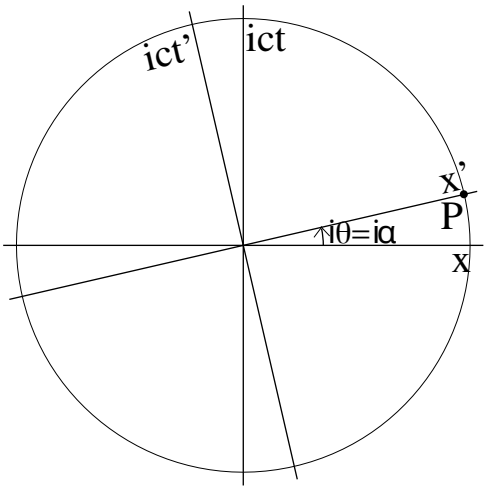

Fig. 10 The S'-axes rotate α counterclockwise to place the x'-axis on the point P. Thus, $\theta = \alpha$.

$$\sin^2 i\theta + \cos^2 i\theta = 1 \tag{21}$$

the expressions for $\cos i\theta$ and $\sin i\theta$ can be obtained from Eq. (20) as functions of v_g:

$$\cos i\theta = \frac{1}{\sqrt{1 - \left(\frac{v_g}{c}\right)^2}} \equiv \gamma \tag{22}$$

$$\sin i\theta = \frac{iv_g/c}{\sqrt{1 - \left(\frac{v_g}{c}\right)^2}} \tag{23}$$

Substituting these above expressions into Eqs. (18) and (19) yields the Lorentz transformations, as originally derived by Minkowski [1]:

$$x' = \frac{x - v_g t}{\sqrt{1 - \left(\frac{v_g}{c}\right)^2}}, \qquad t' = \frac{t - x \cdot v_g/c^2}{\sqrt{1 - \left(\frac{v_g}{c}\right)^2}} \tag{24}$$

where v_g is identified as the relative velocity between the S and S' frames of reference.

The fact that this line of reasoning has led to the Lorentz transformations carries substantial physical significance, as it suggests that relativity is compatible with a universe composed of two opposing natures—physically manifested in terms of space and time—in cyclical alternation, and with the idea that we, as observers, are intrinsically part of the physical world we observe.

4 The circular representation

When the angle is taken to be imaginary, as specified in Eqs. (16)–(17), that representation of the fundamental cycle given by Fig. 7 needs to be updated to its final version: Fig. 11.

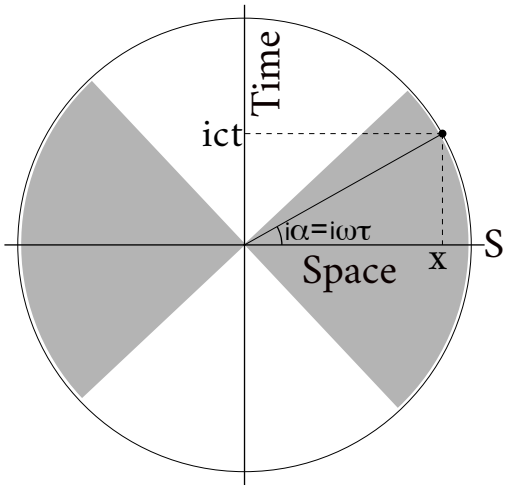

Fig. 11 Shows a generic point P rotating in the spacetime wheel according to its own fundamental cycle. Note that the angular displacement is now explicitly indicated as an imaginary angle and the radius is no longer equal to 1 but allowed to take any other value R. The shaded area represents the observable domain associated with the S reference frame.

Fig. 12 Comparing Eqs. (14)–(15) with the Minkowski rotation and the Lorentz transformation, we observe the presence of two similar triangles.

As it is well known, a particular consequence of introducing the imaginary unit is the breakdown of the direct correspondence between Euclidean geometry and the algebraic values of the magnitudes represented in it. For example, based on the triangle

depicted on the right in Fig. 12, one might expect $v = c$ to occur at an angle $\theta = \pi/4$. However, imposing the condition $v = c$ in the velocity expression given by Eq. (20) leads to the limit $\theta \to \infty$. This illustrates that, once the imaginary unit is introduced, θ can no longer be interpreted as a geometric angle in the Euclidean sense. Instead, it assumes the role of *rapidity*.

This transition reflects a deeper conceptual shift: the moment we adopt an internal viewpoint—that is, the moment we become a constituent of the system—we give up having access to the complete structure (Fig. 5). Indeed, once we perform the transformation $y \to iy$, effectively "entering" the structure, our domain becomes limited to the portion that is real, bounded by infinities and constrained to just two quadrants of the circular diagram (shaded regions in Fig. 11). Nevertheless, we are aware that from an external viewpoint, a broader domain exists beyond these apparent limits. Taking into account this "beyond" is what reinstates the circular nature of the representation.

Therefore, the circular representation remains valid and indeed fundamental because it provides the underlying geometric framework of the physical structure when it is viewed from an external perspective. In this situation, it is worth exploring how the circular representation can still provide valuable insights into the understanding of relativity.

4.1 Some relativistic effects in circular representation

As noted above, the introduction of the imaginary unit breaks the correspondence between the representation of magnitudes in Euclidean geometry and their algebraic values. To analyse this in more detail, we now compare the Lorentz transformation (24) with the expressions that result from the following analysis: if the imaginary unit had not been introduced in (12) and (13), rather than obtaining the Lorentz transformation, the same procedure would have led to:

$$x' = \frac{x + v_g \cdot t}{\sqrt{1 + \left(\frac{v_g}{c}\right)^2}} \qquad t' = \frac{t - x \cdot v_g/c^2}{\sqrt{1 + \left(\frac{v_g}{c}\right)^2}} \tag{25}$$

These expressions represent an alternative formulation of the coordinate transformation given in Eqs. (12)–(13), corresponding to a pure rotation of axes. The change of sign in the numerator, when compared with the Lorentz transformation, implies a reversal of the direction of time.[2] That is, if we aim to represent the Lorentz transformation using a circular interpretation, then time must evolve in the direction opposite to that of the y-axis.[3] On the other hand, the change of sign inside the square roots—acting as a common scaling factor affecting both coordinates—is what breaks the correspondence between geometric and algebraic values.

Let us now examine this more concretely. Fig. 13-*Left* depicts two inertial reference frames S and S' in relative motion, and also their relationship via a rotation

[2] This alteration encodes the Lorentzian signature of the metric tensor.

[3] In our analysis, this may be regarded as preliminary evidence that the negative sign should be taken into account in the transformation (4), leading to $y \to -iy$ and thereby approaching the standard definition of the Wick rotation.

transformation. The reversal of the direction of time becomes evident when considering a body P at rest at the origin of S'. In the upper diagram, as the proper time t' of the body progresses, it appears to move toward positive x in frame S. In contrast, in the circular diagram below, it moves toward negative x as the body ascends along the t'-axis. To reconcile this with the Lorentz transformations, one must interpret time as flowing in the opposite direction—i.e., from top to bottom along the iy'-axis.[4]

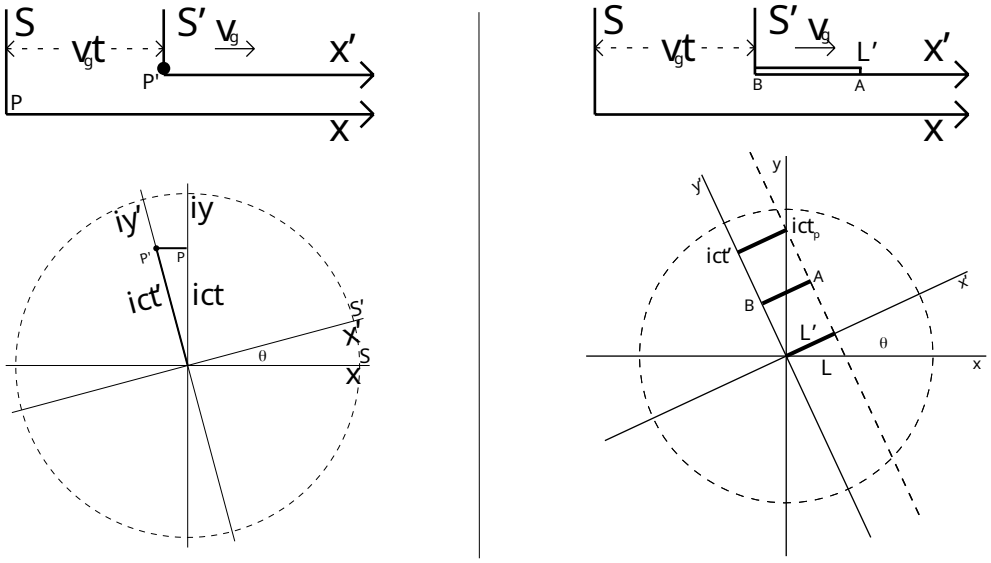

Fig. 13 Left: A body P' is at rest at $x' = 0$ in the frame S', which moves to the right with velocity v_g relative to frame S. Below, the rotation transformation that is assumed to represent, as a first order approximation, the same physical situation. **Right**: A rod of proper length L' is at rest in the S'-frame, with its rear end located at the origin of this frame. The S'-frame moves to the right at velocity v_g relative to the S-frame. Below, a representation of the same situation using a rotation transformation. The time t_p denotes the interval required for the rod to cross the origin of S; the dashed line A represents the passage of the front end, while the solid line B corresponds to the rear end. To make this geometric representation consistent with the Lorentz transformation, one must imagine the rod moving from top to bottom—i.e., under a reversed time flow. This adjustment ensures that the front end of the rod—moving along the dashed line labeled A—crosses the origin of S (i.e., the y-axis) before the rear end, which follows the solid line B.

Despite the time reversal, this circular representation can still be used to derive relativistic effects:

- *Time dilation:* Note that t' and t in Fig. 13-*Left* are geometrically related by means of a projection of the type $t' \cos\theta = t$. However, in order to take into account the introduction of the imaginary unit, the argument in the cosine function needs to be

[4] It is important to emphasize that reversing the time axis in the diagram should not be interpreted as implying a reversal of velocity. If the velocity were also reversed, then the product $v_g \cdot t$ in the first expression of Eq. (25) would remain positive. As a consequence, the minus sign in $x - v_g \cdot t$, which is a defining feature of the Lorentz transformation, would not be recovered.

replaced by its imaginary counterpart. That is,

$$t' \cos(i\theta) = t \quad \Longrightarrow \quad t = \frac{t_0}{\sqrt{1 - v_g^2/c^2}}$$

where Eq. (22) has been used, and t' is identified as the proper time t_0, since point P' is at rest in the S'-frame. Note that the discrepancy between the geometric representation and the corresponding algebraic values: geometrically, $t' > t$, whereas numerically, $t' < t$. This arises from the fact that $\cos(i\theta)$ is a real number greater than one. Therefore, although the geometric representation correctly captures the relationship between t and t' as a projection, their algebraic values differ in reality.

- *Length contraction:* Consider Fig. 13–*Right*, where a rod of proper length L', positioned with its rear end at the origin of the S'-frame is observed to move at velocity v_g relative to the S-frame. Again, the geometric relation between L and L' can be derived by means of a simple projection:

$$L' = L \cos i\theta \quad \Longrightarrow \quad L = L_o \sqrt{1 - v_g^2/c^2}$$

where L' was identified as the proper length L_o since the rod is at rest in S'.

- *Gravitational time dilation:* Fig. 14 illustrates the same rod depicted in Fig. 13–*Right*, which initially moves at a constant velocity. Once the rear end of the rod passes the origin of the S-frame, the rod begins to accelerate uniformly with constant proper acceleration.
  The constant proper acceleration causes the dashed trajectories (representing the motion of the rod's endpoints) to curve with a constant radius of curvature: the rear end B follows a path with radius $R - L'$, while the front end A follows a path of radius R. Consequently, the corresponding arc lengths S_B and S_A differ, and their ratio is given by:

$$\frac{S_B}{S_A} = \frac{R - L'}{R}$$

  Since a spatial length in this framework is proportional to a proper time interval τ, we can write:

$$\frac{\tau_B}{\tau_A} = \frac{R - L'}{R} = \frac{\omega_A}{\omega_B} \tag{26}$$

  Finally, due to the Equivalence Principle in GR, the above result also applies to two clocks situated at different heights within a uniform gravitational field of intensity $g = c^2/R$, with $h_A > h_B$ and vertical separation $L' = h_A - h_B$. This expression will be used later.

Thus, the geometric method developed here basically consists of two pairs of axes with a relative rotation, which represent two inertial frames of reference, and the use of the $\sin i\theta$ and $\cos i\theta$ functions to make projections in the same way that the normal sine and cosine do in Euclidean geometry. Therefore, although the introduction of the imaginary unit modifies the Euclidean metric, the structure of the Minkowski rotation

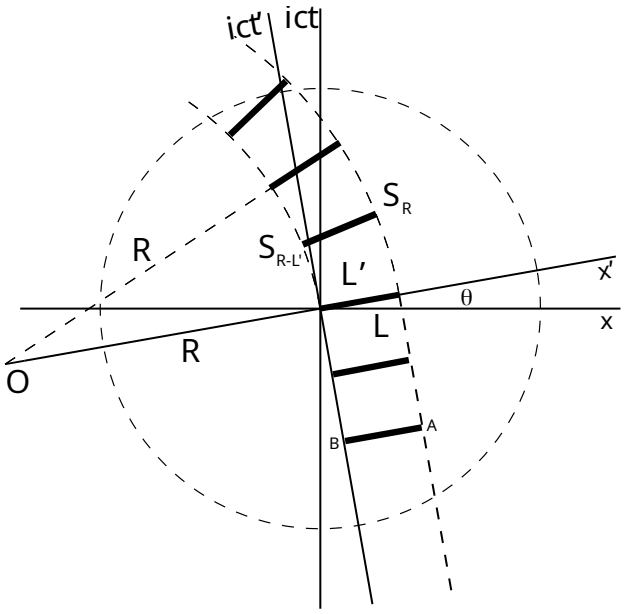

Fig. 14 Shows an accelerating rod in circular representation: the rear end follows the arc S_B, while the front end traces S_A. As previously discussed, achieving consistency between rotational and Lorentz transformations requires incorporating a reversal of time. However, as the figure shows, reversing time also implies a deceleration of the rod rather than an acceleration, which does not reflect the physical situation described initially. Nonetheless, if time reversal is assumed to not affect the sign of velocity, this figure remains valid as a representation of an accelerating rod, even though the diagram can no longer be made visually consistent with the Lorentz transformation, as time reversal alters the underlying physical scenario.

remains fundamentally circular, and the relationships between the various quantities involved can still be represented within a circular framework.

5 Harmonic Reinterpretation of Relativity

Although the circular representation of the relativistic phenomena discussed above—Figs. 13-14—serves as a useful tool for deriving the corresponding mathematical expressions, it does not capture the dynamical nature of the fundamental cycle. To incorporate this aspect and explore its consequences, we return to the earlier depiction of the fundamental cycle shown in Fig. 11. We now ask whether this representation—together with the use of $\cos(i\omega\tau)$ and $\sin(i\omega\tau)$ for performing projections—can be employed to derive the equations of relativistic dynamics.

5.1 The fundamental cycle and the laws of relativity

It is natural to assume that the linear velocity of point P in Fig. 11 in its circular motion through spacetime is equal to the speed of light c. Indeed, under this

assumption, the corresponding angular frequency is given by

$$\omega = \frac{c}{R} \tag{27}$$

and taking the derivative of Eq. (17) with respect to τ then yields[5]

$$\frac{dt}{d\tau} = \gamma \tag{28}$$

which is a well-known result in relativity, provided that τ is interpreted as the proper time. Thus, let the linear velocity in the fundamental cycle be the speed of light, such that the time variable τ can be identified with the proper time.

The projection of the circular motion of point P onto the x-axis yields a type of *complex Simple Harmonic Motion* (SHM*), from which the *proper velocity* v_τ and *proper acceleration* a_τ can be obtained by differentiating x, as defined in Eq. (17), with respect to the proper time τ:

$$x(\tau) = R\cos(i\frac{c}{R}\tau) \tag{29}$$

$$v_\tau(\tau) = \frac{dx}{d\tau} = -ic\sin\left(i\frac{c}{R}\tau\right) \tag{30}$$

$$a_\tau(\tau) = \frac{d^2x}{d\tau^2} = \frac{c^2}{R}\cos\left(i\frac{c}{R}\tau\right) \tag{31}$$

Nevertheless, do v_τ and a_τ have any physical meaning? Indeed, one realises that multiplication on both sides of (30) by a rest mass m_o leads to the expression of the relativistic momentum:

$$m_o v_\tau = -im_o c\sin\left(i\frac{c}{R}\tau\right) = \frac{m_o v_g}{\sqrt{1-(v_g/c)^2}} \equiv p, \tag{32}$$

where (20) was used. Moreover, differentiating the momentum with respect to t one encounters the force:

$$F \equiv \frac{dp}{dt} = \frac{dp/d\tau}{dt/d\tau} = \frac{m_o\frac{c^2}{R}\cos\left(i\frac{c}{R}\tau\right)}{\cos\left(i\frac{c}{R}\tau\right)} = m_o\frac{c^2}{R}, \tag{33}$$

which turns out to be a constant value. Thus, multiplying by x on both sides one would expect to find out an energy expression:

$$E \equiv F\cdot x = \frac{m_o c^2}{R}x = m_o c^2\cos\left(i\frac{c}{R}\tau\right) = \frac{m_o c^2}{\sqrt{1-(v_g/c)^2}}, \tag{34}$$

which, indeed, is the relativistic energy. Therefore, the projection of the fundamental cycle onto its real axis produces a complex Simple Harmonic Motion (SHM*) whose

[5] The derivatives of the sine and cosine of an imaginary angle are: $(\cos i\theta)' = -i\sin i\theta$ and $(\sin i\theta)' = i\cos i\theta$.

velocity and acceleration are directly proportional to the relativistic momentum and energy.

Note that, although the p and E expressions (32) and (34) do not show up explicitly the dynamics of the cycle, the force (33) does, since its associated acceleration c^2/R is clearly centripetal. Moreover, according to GR, this acceleration corresponds to gravity $g = c^2/R$ whenever R is interpreted as the radius of curvature of spacetime. Therefore, if R in Fig. 11 is assumed to be so, then the proper acceleration felt by the P-point while turning around in the wheel of spacetime should be none other than gravity:

$$a_\tau(\tau = 0) = \frac{c^2}{R} \equiv g \tag{35}$$

Joining results, one has

$$t = \frac{-i}{c} R \sin\left(i\frac{c}{R}\tau\right) \tag{36}$$

$$x = R\cos\left(i\frac{c}{R}\tau\right) = R\frac{dt}{d\tau} \tag{37}$$

$$p = -im_o c \sin\left(i\frac{c}{R}\tau\right) = m_o\frac{dx}{d\tau} = m_o v_\tau \tag{38}$$

$$E = m_o c^2 \cos\left(i\frac{c}{R}\tau\right) = m_o R\frac{d^2x}{d\tau^2} = m_o a_\tau R \tag{39}$$

in which the expressions for momentum and energy take on a remarkably natural form, suggesting an interesting coexistence between relativity, Newtonian mechanics and harmonic motion.

It is worth noting that, from the point of view of point P in Fig. 11—that is, from its proper reference frame, corresponding to $\tau = 0$ in the expressions above—its momentum is zero. On the other hand, since P is undergoing continuous circular motion within the spacetime wheel at a linear velocity equal to c, this motion gives rise to a centripetal acceleration—interpreted as gravity—given by Eq. (35), which, when substituted into Eq. (39), leads directly to the expression $E = m_0c^2$. Thus, although commonly referred to as rest energy, this quantity arises from the spacetime rotation. In this sense, we shall see in the following section that the rest energy can be interpreted as a form of elastic potential energy.

Finally, by applying systematically the trigonometric relation (21) to expressions (36)-(39) one obtains, apart from the E-p-relation, two additional expressions:[6]

$$E^2 = (cp)^2 + (m_o c^2)^2 \tag{40}$$

$$\boxed{\begin{aligned} \frac{x^2}{R^2} &= 1 + \frac{p^2}{m_o^2 c^2} \qquad (41)\\ E^2 &= \frac{m_o^2 c^6 t^2}{R^2} + (m_o c^2)^2 \qquad (42) \end{aligned}}$$

[6]These expressions remain valid throughout the entire circular domain, as Eq. (21) holds even when the argument of the sine and cosine functions is a general complex number z; that is, even in the regime where $v > c$.

The first two are, respectively, the analogues of the a–v and x–v relations from classical Simple Harmonic Motion (SHM):

$$a^2 = -(\omega v)^2 + (R\omega^2)^2$$
$$\frac{x^2}{R^2} = 1 - \frac{v^2}{R^2\omega^2}$$

The sign differences arise from the presence of the imaginary unit in this relativistic framework. In this context, ω must be replaced by c/R, and the classical variables v and a by their corresponding expressions in terms of p and E, as given in Eqs. (38) and (39).

The second expression, Eq. (41), is particularly noteworthy as it establishes a direct relation between the spatial coordinate x of a rotating particle in spacetime and its relativistic momentum p, scaled by the curvature radius R and the rest mass m_o. Notably, this equation links the spatial separation of the particle from an observer to its momentum content. In a broader physical context, it may be interpreted as connecting the distance to an astronomical object with its recession momentum. Thus, this relationship reflects the cosmological implications of the fundamental cycle, which appears to naturally incorporate recession phenomena—such as those observed in the expansion of the universe—as an intrinsic feature of its underlying geometrical structure.

In contrast, Eq. (42) possesses no classical analogue and again reflects the cyclic geometry of spacetime.

Eqs. (41) and (42) are, to the best of the author's knowledge, novel results. They emerge naturally from the fundamental cycle and may offer new insight into the structure of relativistic dynamics.

5.2 The complex harmonic oscillator

In classical physics, the Lagrangian is defined as the difference between kinetic and potential energy, $L = T - V$. In relativity, however, the Lagrangian of a free particle takes a markedly different form: $L_r = -m_0c^2\sqrt{1 - v^2/c^2}$, where no trace of the classical definition seems apparent. Nevertheless, we will now demonstrate that this expression can still be interpreted, in essence, as kinetic energy minus potential energy.

If the complex Simple Harmonic Motion (SHM*) that results from projecting the rotation of the point P in Fig. 11 onto the x-axis is assumed to be performed by an harmonic oscillator of mass m_o and elastic constant k—as depicted in Fig. 15—, then its associated frequency of oscillation could still satisfy the classic expression

$$m_o\omega^2 = k \tag{43}$$

Let us assume that it is so. Then, if the angular frequency of spacetime rotation $\omega = c/R$ is substituted here, the result is twice the energy conservation expression of the classic harmonic oscillator:

$$m_oc^2 = kR^2 \tag{44}$$

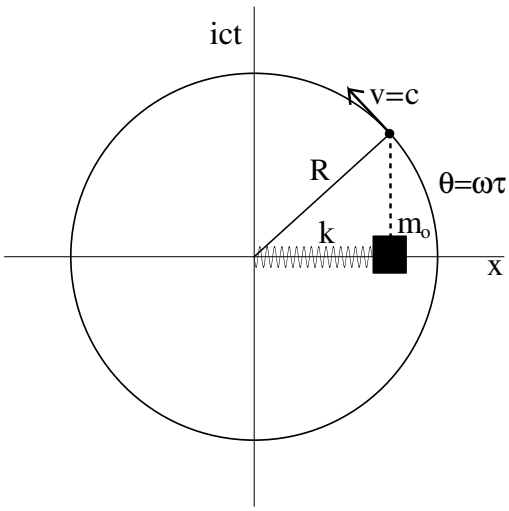

Fig. 15 If the fundamental cycle is projected onto the spatial axis, it yields a complex Simple Harmonic Motion (SHM*), which is here interpreted as the motion of a harmonic oscillator with mass m_o and spring constant k.

where here c represents the maximum velocity and R the maximum amplitude of vibration. By dividing both sides of the E–p relation (40) by kR^2, and noting that, according to Eqs. (29) and (44), the energy in Eq. (39) can be written as $E = Rkx$, we obtain:

$$\frac{(Rkx)^2}{kR^2} - \frac{(cp)^2}{kR^2} = \frac{k^2R^4}{kR^2} \quad \Rightarrow \quad kx^2 - \frac{p^2}{m_o} = kR^2.$$

This final expression is precisely twice that of the classical harmonic oscillator Lagrangian. Consequently,

$$T' - V' = -m_oc^2 \quad \Rightarrow \quad L' = -m_oc^2,$$

where T' and V' denote twice the classical kinetic and potential energies, respectively. Therefore, the Lagrangian L' remains constant when a particle travels through space-time, i.e. when τ evolves linearly according to inertial motion. Thus, one can write the following expression for the action

$$S = \int_{\tau_1}^{\tau_2} L'\, d\tau = \int_{t_1}^{t_2} -\frac{m_oc^2}{\gamma}\, dt = -m_oc^2\Delta\tau \tag{45}$$

from where the relativistic Lagrangian is identified: $L = -m_oc^2/\gamma$. Therefore, based on this simple analysis, several key conclusions can be drawn:

1. A direct equivalence is established between inertial motion and rotation in space-time. In other words, a particle that follows its fundamental cycle is a free particle.

2. The fact that this procedure yields a well-known expression—namely, the relativistic Lagrangian for a free particle—supports the validity of Eq. (43) even in the context of complex Simple Harmonic Motion (SHM*).
3. Thus, the fundamental cycle is associated with a value of the elastic constant k: given the mass m_0 and the angular frequency ω, Eq. (43) determines the unique value of k that ensures harmonic behavior.
4. Given the universality of the fundamental cycle, it follows that the behavior of the universe itself may be governed by this value of k, suggesting an analogy with the cosmological constant Λ in GR. This raises the possibility of a conceptual or mathematical relationship between these two constants.
5. As in Section 2, where the relativistic invariant interval $x^2 - (ct)^2 = R^2$ was interpreted as an "internal view" of the geometry of the circle, now the E-p-relation (40) can be interpreted as an internal view of the conservation of energy in the classical harmonic oscillator.

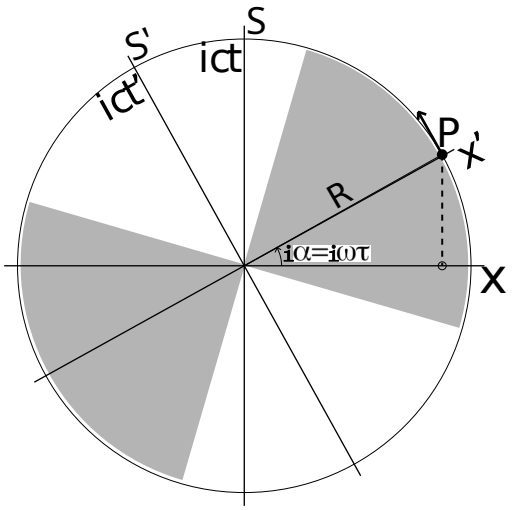

Fig. 16 A point P' is at rest in the reference frame S'. This frame rotates in spacetime with angular velocity ω relative to a rest frame S, which represents flat spacetime. In S', the point P' has no linear momentum, yet due to its rotational motion at a radius R, it experiences a centripetal acceleration—interpreted as a gravitational effect—ultimately giving rise to the rest energy $E = m_0c^2$ measured in S'. The shaded area represents its observable domain.

6. This analysis also suggests a novel interpretation of rest energy and gravity:

   Although from the perspective of the reference frame S the point P undergoes a SHM*, from P's proper axes, the body perceives itself as being in a state where the value of x is always maximal—geometrically speaking, not algebraically—and equal to R. In this configuration, since there is no radial motion, its associated linear momentum is zero. However, the fact that it is rotating implies the presence of a corresponding centripetal acceleration—or gravity—, which endows the body with a form of energy: the rest energy. This scenario is analogous to a harmonic oscillator displaced from equilibrium due to rotational motion. Imagine a mass attached to

a spring, rotating at constant angular velocity on a horizontal plane, as illustrated in Fig. 17. The spring stretches to a fixed distance R. Since the radius of rotation remains constant, the system is radially at rest (i.e., zero relativistic momentum). However, the displacement of the mass by a distance R from the equilibrium point leads the spring to exert a constant centripetal force equal to m_0c^2/R, which we interpret as the gravitational force. Consequently, the work accumulated by this constant force corresponds to the rest energy $E = m_0c^2$.[7]

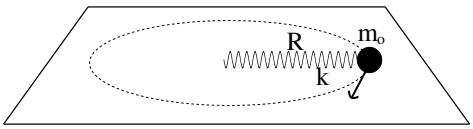

Fig. 17 A body of mass m_0 attached to a spring with elastic constant k rotates uniformly on a horizontal plane. Due to the centrifugal effect of the rotation, the spring extends to a length R. In this analogy, the rest energy is interpreted as the elastic potential energy stored in the spring. Furthermore, since the radius remains constant during the motion, the radial velocity is zero, and therefore the relativistic linear momentum is also zero.

5.3 The 8 phases of the fundamental cycle

By combining Eqs. (14)–(15) with Eqs. (29)–(31), the position, proper velocity, and proper acceleration can be expressed as

$$x(\tau) = R\frac{x}{\sqrt{x^2 - y^2}} \tag{46}$$

$$v_\tau(\tau) = c\frac{y}{\sqrt{x^2 - y^2}} \tag{47}$$

$$a_\tau(\tau) = \frac{c^2}{R}\frac{x}{\sqrt{x^2 - y^2}} \tag{48}$$

These expressions reveal that the respective quantities alternate between real and imaginary values, and also change sign throughout the fundamental cycle. Fig. 18 illustrates how this alternation divides the cycle into eight distinct regions, while Fig. 19 presents the same structure in a more schematic way. As can be observed, despite the formal analogy with SHM, the SHM* differs fundamentally from the familiar expansion–contraction dynamics, which comprises only four distinct phases. The values of the velocity and acceleration are particularly noteworthy, as they are proportional to the momentum and energy, respectively. Note that half of these phases are real in nature, while the other half are imaginary, as indicated by the black and red regions in Fig. 19-*Right*. The infinities act as gatekeepers between the real and imaginary regions and should be regarded as mathematical singularities—as is often the case in QFT—rather than physical impossibilities.

[7] Interestingly, rather than evaluating the force throughout the interval from the origin ($x = 0$) to R, only its value at $x = R$ is considered.

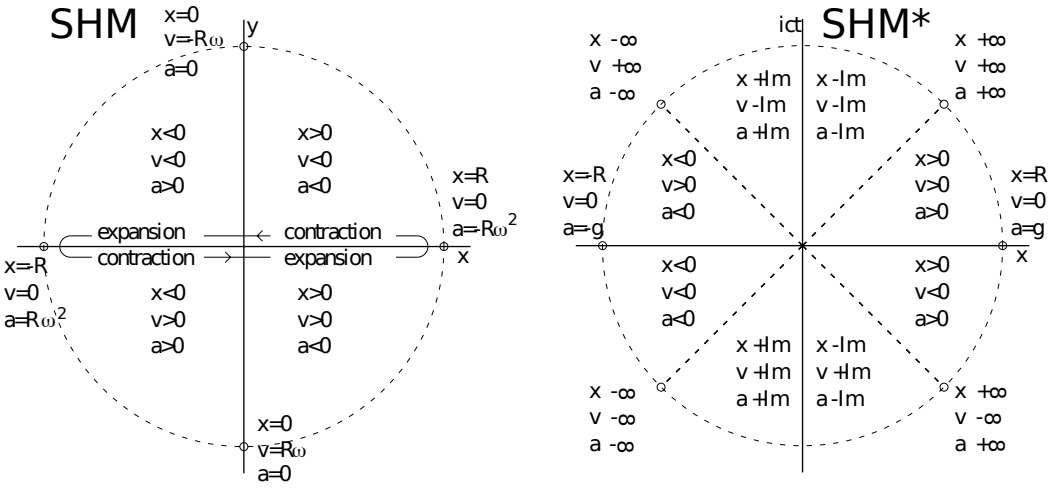

Fig. 18 **Left:** Depicts the position, velocity, and acceleration of the classical SHM in each quadrant, including at $x = 0$ and $t = 0$. This corresponds to the familiar spring-like oscillation. For example, in the first quadrant, the system undergoes contraction: position is positive ($x > 0$), velocity is negative ($v < 0$), and acceleration is also negative ($a < 0$). **Right:** In contrast, complex SHM (SHM*) features eight distinct regions, within which the values of x, v_τ, and a_τ—given by Eqs. (46)-(48)—can be either real or imaginary. Some divergences occur at the boundaries of these regions. At $t = 0$, the acceleration corresponds to the "proper" gravitational acceleration: $g = c^2/R$. For example, in the first half quadrant, where $x > 0$, $v > 0$ and $a > 0$, the system undergoes and accelerated expansion.

These eight stages represent the complete sequence a particle undergoes during one full fundamental cycle; that is, while remaining in its inertial state. The radical differences between stages suggest that the fundamental cycle can be interpreted as a process of transformation—a succession of dynamical states where the spacetime fabric undergoes a cycle of mutations or physical phases.

In particular, in the second quadrant of Fig. 19-*Right*—which corresponds to the domain where $v_g > c$, and hence lies beyond the domain of special relativity and the observable world—the quantities associated with time, position, momentum, and energy become imaginary.[8] In this context, the arguments of expressions (36)–(39) can be written as $i\theta + \pi/2$, leading to the following relations:

$$t_{II} = \frac{-i}{c} R \sin\left(i\frac{c}{R}\tau + \frac{\pi}{2}\right) = \frac{-i}{c} R \cos\left(i\frac{c}{R}\tau\right) \tag{49}$$

$$x_{II} = R \cos\left(i\frac{c}{R}\tau + \frac{\pi}{2}\right) = -R \sin\left(i\frac{c}{R}\tau\right) \tag{50}$$

$$p_{II} = -im_0 c \sin\left(i\frac{c}{R}\tau + \frac{\pi}{2}\right) = -im_0 c \cos\left(i\frac{c}{R}\tau\right) \tag{51}$$

[8] This superluminal or tachyonic domain has been the subject of several theoretical investigations aimed at extending the framework of special relativity to accommodate faster-than-light phenomena [23–26]. These approaches suggest that, although imaginary-valued quantities may not be directly observable, they may reflect deeper layers of physical law accessible through analytic continuation or extended relativistic frameworks—precisely the kind of structure that underlies the circular representation developed in this paper.

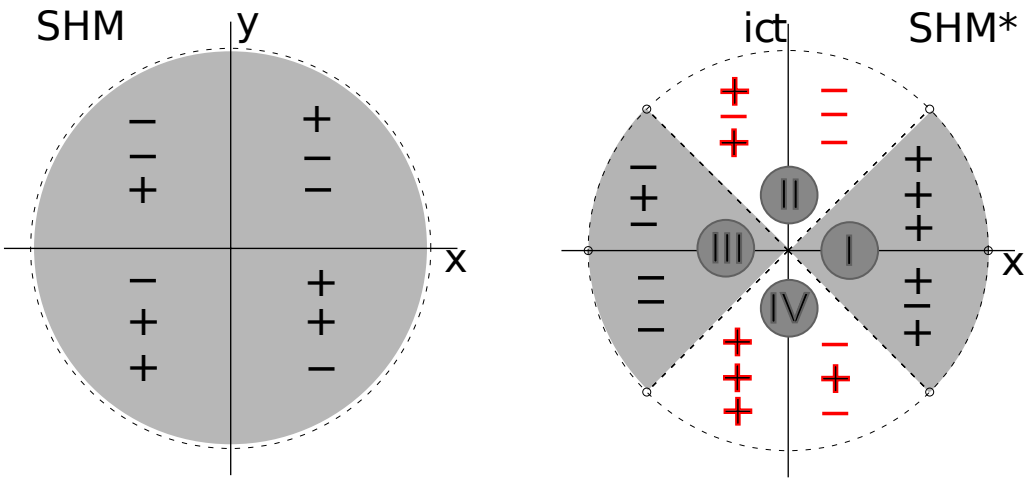

Fig. 19 **Left:** Simplified representation of the signs of position, velocity, and acceleration in each quadrant of the classical simple harmonic motion (SHM). **Right:** The analogous case for the modified complex representation, referred to as SHM*. Signs in red denote imaginary quantities. Notably, no combination of signs in SHM* matches those in the classical case. This highlights a fundamental difference: whereas classical SHM describes a cyclic process of expansion and contraction, SHM* exhibits no such analogy. Additionally, it is emphasized that the proper time τ evolves in a counterclockwise circular path, while the coordinate time t oscillates along the y-axis. In particular, t increases in the first quadrant but reverses direction in the third quadrant.

$$E_{II} = m_0c^2 \cos\left(i\frac{c}{R}\tau + \frac{\pi}{2}\right) = -m_0c^2 \sin\left(i\frac{c}{R}\tau\right) \tag{52}$$

By applying analogous transformations to the remaining quadrants, the complete set of results summarized in Table 1 is obtained.

	I	**II**	**III**	**IV**
ϕ	$i\theta$	$i\theta + \frac{\pi}{2}$	$i\theta + \pi$	$i\theta + \frac{3\pi}{2}$
ict/R	$\sin(i\theta)$	$\cos(i\theta)$	$-\sin(i\theta)$	$-\cos(i\theta)$
x/R	$\cos(i\theta)$	$-\sin(i\theta)$	$-\cos(i\theta)$	$\sin(i\theta)$
$\frac{p}{m_0c} = \frac{dx}{d\theta}$	$-i\sin(i\theta)$	$-i\cos(i\theta)$	$i\sin(i\theta)$	$i\cos(i\theta)$
$\frac{E}{m_0c^2} = \frac{d^2x}{d\theta^2}$	$\cos(i\theta)$	$-\sin(i\theta)$	$-\cos(i\theta)$	$\sin(i\theta)$

Table 1 Normalized values of time, position, momentum and energy on the hyperbolic unit circle and their first and second derivatives with respect to the real parameter θ—which stands for $(c/R)\tau$—, defined over the domain $-\pi/4 < \theta < \pi/4$.

The third quadrant is characterized by negative energy values and, notably, by the fact that—as the fundamental cycle progresses—the coordinate time t evolves in reverse. This behavior is consistent with Feynman's interpretation of antiparticles [4, 27], where they are understood as particles possessing negative energy and propagating backward in time.

The second and fourth quadrants correspond to regions beyond the scope of direct physical observation. To provide an interpretation of these domains, we propose the following intuitive argument.

Previously, we interpreted the Wick rotation—Eq. (4)—as the transformation that transitions us from being external observers of the physical system to becoming intrinsic constituents of it. Once this transformation is applied—placing us within the internal viewpoint—an inaccessible region of imaginary nature emerges: the domain of absence or the beyond. Although it constitutes an inconceivable domain, it borders the real world. This implies that, in some way, observing this boundary may provide us with an external perspective on an otherwise inaccessible realm.

If we apply the Wick rotation a second time, we effectively perform an internal view of the internal view. And just as the imaginary of the imaginary yields the real ($i \cdot i = -1$), the internal perspective of the internal must correspond to an external perspective. However, in this case, the negative sign implies that this external viewpoint appears rotated or inverted. As illustrated in Fig. 20, this conceptual inversion implies that the real manifestation of the imaginary phases shown in Fig. 19-*Right* must be sought in the opposite semi-quadrants of Fig. 19-*Left*.

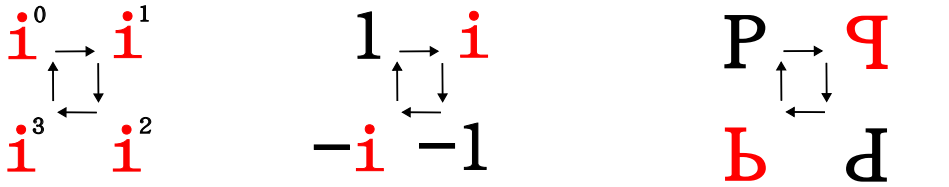

Fig. 20 Left and Center: Successive powers of the imaginary unit (1, i, -1, $-i$) are represented in a cyclic configuration. **Right:** Multiplication by i is interpreted geometrically as a mirror transformation. Multiplication by i^2 corresponds to two consecutive reflections across orthogonal axes. Under this interpretation, the cyclical nature of the powers of i finds a geometric analogue in the transformations among the letters p, q, b, and d. For instance, p and q are related via a vertical mirror, whereas q and d are related via a horizontal mirror. Consequently, p and d are connected through two orthogonal reflections, equivalent to a 180° rotation. In this framework, a single mirror transforms a real component into an imaginary one (or vice versa), while two consecutive reflections yield a sign reversal or half-turn rotation.

Based on this interpretation, the associations are shown in Fig. 21-*Left*, and the complete outcome is presented on its right. The resulting structure reveals a fundamental cycle consisting of eight distinct phases, each possessing a real manifestation. Interestingly, these eight stages correspond to all possible combinations of the signs of position, velocity, and acceleration. This suggests the simple change in nomenclature depicted in Fig. 21-*Right*, which connects this analysis with the cycle of transformation found in the cosmological system of classical Chinese thought. Given the structural parallelism, it would be of considerable interest to investigate whether this ancient cosmological framework could offer a qualitative explanation of the various phases of the fundamental cycle.

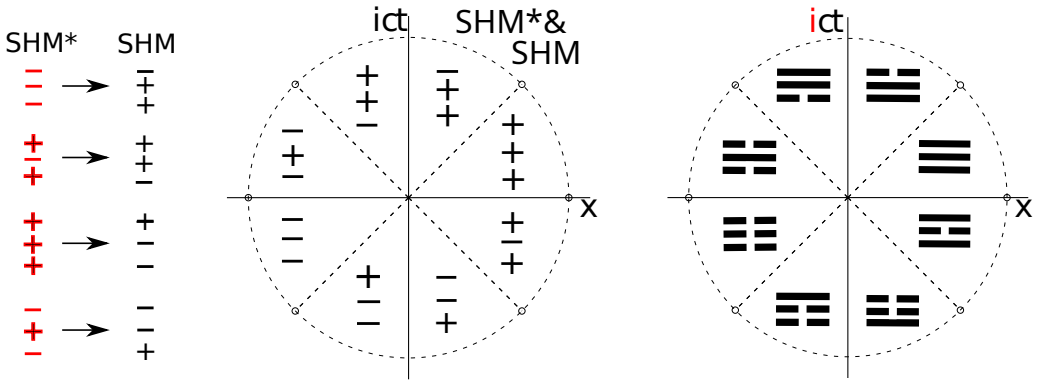

Fig. 21 **Left:** This panel shows the different combinations of signs involving imaginary values (highlighted in red in Fig. 19) and their proposed correspondence with real values. This association arises from the assumption that the imaginary values of the SHM* manifest as real quantities, based on the notion that the imaginary of an imaginary is real. Furthermore, this real manifestation must correspond to the classical SHM, which represents the external view. **Center:** With this correspondence, the fundamental cycle comprises eight distinct phases with real manifestations, each representing one of the eight possible combinations of signs for position, velocity, and acceleration. **Right:** Shows the *bagua* that results by changing the positive signs with solid lines and negative signs with broken lines.

6 A Harmonic Cosmological Model

If we allow a body to fall indefinitely through a tunnel drilled straight through the Earth (neglecting Earth's rotation, translation, and air resistance), it would fall vertically downward, cross the center of the Earth at high speed, then decelerate until it would momentarily stop at the opposite end—only to fall again, repeating the process endlessly (Fig. 22-*Left*).

To simplify matters, let us assume that the periodic motion of the falling object can be modeled as a SHM—a clearly unrealistic approximation. This SHM can, in turn, be described as the projection of a UCM onto the vertical axis, as shown in Fig. 22-*Right*.

Now, if instead of a single body we were to drop two, with a certain time delay between them, both would fall and oscillate through the tunnel, crossing paths with opposite velocities. Throughout the cycle, various situations of relative motion between the two bodies would emerge. If this relative motion were observed from body A, for instance—which clearly constitutes a non-inertial frame—we would find ourselves in a linear circuit, constantly accelerating and decelerating, always chasing body B ahead of us, yet never quite catching up.

Since SHM comprises four distinct regimes (Fig. 19-*Left*), we can place body A in four positions and body B in four corresponding ones, giving a total of $4 \cdot 4 = 16$ distinct relative-motion configurations between A and B.[9]

This situation—albeit highly idealized and physically unrealistic—serves as an introduction to the cosmological model that arises from the fundamental cycle.

To proceed, we must first construct the relativistic equivalent of this situation, which is none other than two points rotating in the spacetime wheel with the same

[9]Not considering which of the bodies is ahead when they occupy the same quadrant.

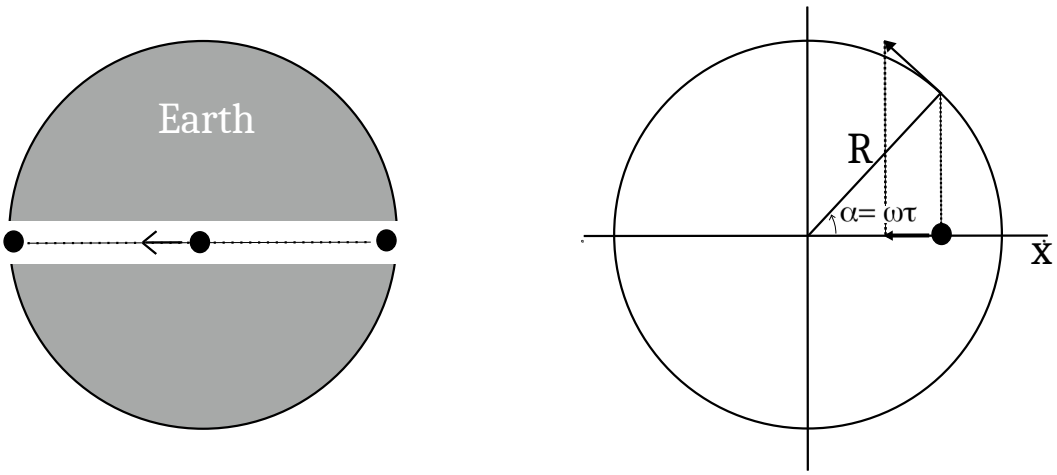

Fig. 22 **Left:** A body falls into a hole drilled through the Earth. **Right:** Its motion is approximated as simple harmonic motion (SHM), understood as the projection of uniform circular motion (UCM). The radius R here corresponds to the Earth's radius.

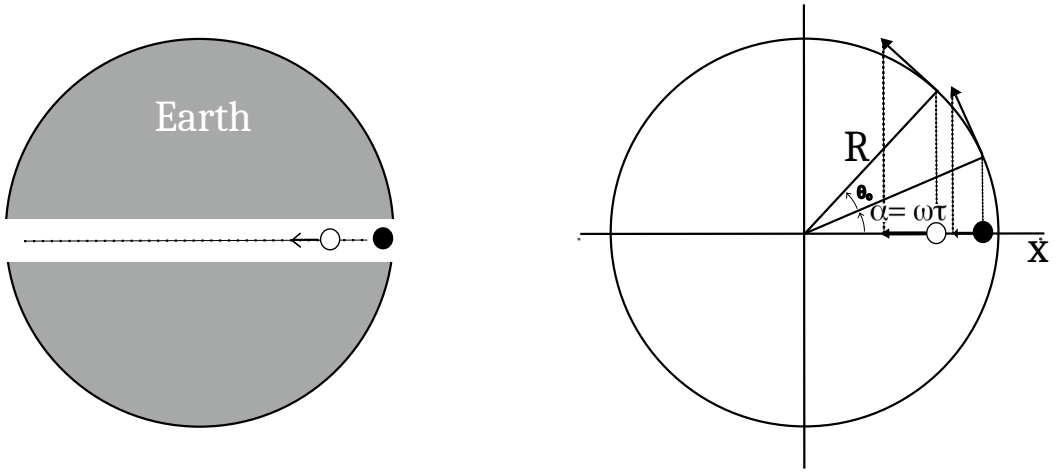

Fig. 23 **Left:** Two bodies falling through the tunnel that passes through the Earth. **Right:** Their respective motions are modeled as two phase-shifted SHMs, separated by an angle θ_o.

radius and angular velocity, such that the projection of their motion onto the x-axis produces two SHM* curves differing only in phase, as depicted in Fig. 24. This is the relativistic analogue of the two bodies in free fall through the tunnel.

However, despite the common underlying structure, it is important to recognize that, in the relativistic case, space and time measurements are relative to the observer. This requires us to explicitly define the proper reference frames for each body, as shown in the figure, where S' refers to the coordinate system in which A is stationary,

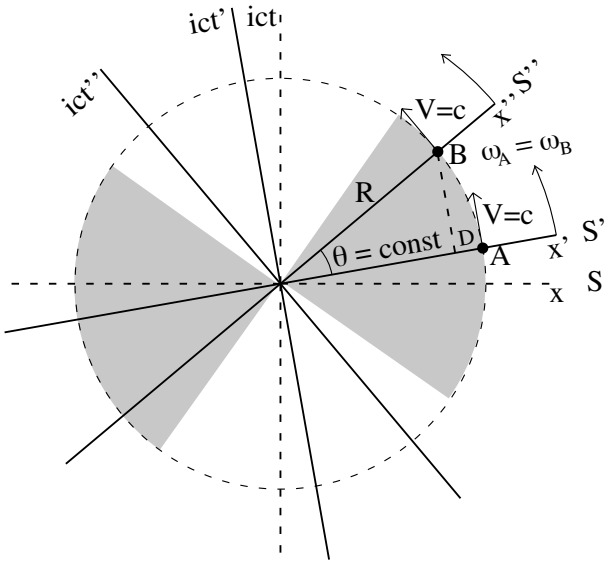

Fig. 24 This figure represents the same situation as Fig. 23-*Right*, but now interpreted in terms of two galaxy clusters A and B rotating within the spacetime wheel, with a curvature radius R equal to the global radius of the universe. In this context, it is necessary to define the reference frames S' and S'' centered on each body in order to introduce their respective time coordinates, in addition to a fixed coordinate system S. On the other hand, the projection of these circular motions onto the x-axis yields the characteristic SHM* of relativistic dynamics, as opposed to the conventional SHM. The distance D represents the amount by which the radius of curvature of B has been reduced from the point of view of A. It can also be interpreted as the distance at which an object must lie in order to have a recession velocity equal to v_g, as defined in Eq. (20). The shaded region designates the observable domain for observer A.

S'' to that of B, and S to the non-rotating system representing flat spacetime.[10] This distinction in reference frames will also lead to a significantly different perception that A has of B, compared to the original free-fall scenario.

We shall therefore consider the Universe to be composed of a set of freely falling objects—namely, bodies orbiting along the 'wheel' of spacetime—where the radius R no longer represents the radius of the Earth, but rather that of the Universe itself, and where the objects in question are now the largest bound structures, such as galaxy clusters.

Under this assumption, if we place ourselves at body A, the way in which we perceive body B corresponds to how galaxy clusters are observed from our own perspective. This provides us with a concrete vision of the cosmos.

To determine precisely how point A perceives point B throughout the fundamental cycle, one must consider how Newton's second law appears from the perspective of an observer seated in the rotating frame S', which is clearly non-inertial. Temporarily disregarding the imaginary and temporal nature of the y-axis, classical mechanics tells us that Newton's second law in the rotating frame depicted in Fig. 25 becomes [28]:

[10] Indeed, from Eq. (27), $\omega = 0$ implies $R \to \infty$.

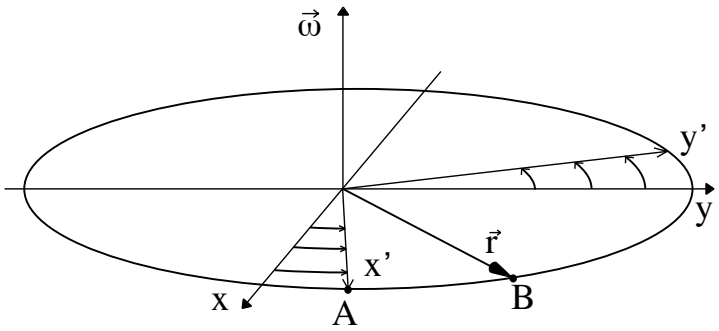

Fig. 25 Depiction of a reference system S' rotating with angular velocity $\vec{\omega}$ with respect to a fixed frame S. Points A and B are stationary in S'.

$$m\vec{a'} = \vec{F} - 2m\vec{\omega} \times \vec{v'} - m\dot{\vec{\omega}} \times \vec{r} - m\vec{\omega} \times (\vec{\omega} \times \vec{r}) \tag{53}$$

This equation includes three fictitious forces, referred to from left to right as the *Coriolis force*, *Euler force*, and *centrifugal force*. In our scenario, where body B remains at rest in the rotating frame S' and ω is constant, both the Coriolis and Euler forces vanish, leaving only the centrifugal force. Substituting $\omega = c/R$ yields, in magnitude, a gravitational acceleration of c^2/R. This aligns with the interpretation in GR, where gravity is regarded as a fictitious force arising from the non-inertial nature of the reference frame.

To resolve the general relativistic case of interest here, one would need to modify the above equation by transforming the y-axis as $y \to ict$, as suggested in equation (7),[11] and potentially allow body B to be non-stationary in S', which could give rise to relativistic analogues of the Coriolis and Euler forces [29]. Proceeding in this way, it may turn out, for instance, that what physics has identified as dark matter or dark energy is nothing but the effect of these fictitious forces arising from the non-inertial nature of our own reference frame.

However, to make progress more straightforwardly, we shall instead highlight phenomena that already emerge without solving the full equation.

6.1 Gravitational Interpretation of Redshift and Hubble's law

The harmonic model of the universe provides explicit expressions for the recession velocity and acceleration. Although the S frame in Fig. 26-*Right* offers a broader perspective, we, as observers embedded within the structure, are inherently confined to the viewpoint of point A, i.e., to the rotating reference frame S'.

Within our observable domain—the shaded region in the figure—body B exhibits a positive velocity (it recedes from the observer)[12] given by Eq. (20), and also experiences

[11] Or $y \to -ict$.
[12] Body C recedes in the opposite direction to that of B.

acceleration:

$$a_g = \frac{dv_g}{dt'} = \frac{dv_g/d\theta}{dt'/d\theta} = \frac{c(\cos i\theta)^{-2}}{\frac{R}{c}\cos i\theta} = \frac{c^2}{R}\left(1 - \frac{v_g^2}{c^2}\right)^{3/2} = \frac{a_\tau}{\gamma^4} \tag{54}$$

However, this is a rather peculiar scenario because, according to Fig. 26-*Right*, despite the presence of acceleration, the velocity remains constant as θ does not change with the passage of proper time τ, and, despite the velocity, the distance D also remains constant. How is this possible?

Although this may seem contradictory, it is a situation we have already encountered in the case of the falling rod with constant acceleration. Indeed, as depicted in Fig. 26-*Left*, the emitter B and the receiver A always share the same instantaneous velocity. However, during the time it takes for a light signal to propagate from B to A, the rod accelerates. Specifically, the velocity increases by gt, where t is the light travel time across the distance D, which is approximately D/c.

Hence, by the time the signal reaches A, the rod has increased its velocity by approximately gD/c. This is the velocity the receiver possesses relative to the emitter at the moment of signal reception. Thus, we find a situation in which the receiver at point A experiences the illusion that body B is continuously receding with increasing velocity—i.e., accelerating—when in fact both the proper separation D and the relative velocity v_g remain constant.

Within this framework, Hubble's law [30] can be interpreted geometrically, as illustrated in Fig. 26-*Right*. Indeed, as cosmic observers, we are located at point A and revolve within the spacetime wheel of the universe at a global curvature radius R, along with other galaxy clusters such as B and C, which are at a distance D from us and lie within our observable domain—characterized by recession velocities lower than c. Although from the perspective of the fixed coordinate system S, bodies B and C revolve with radius R, from our point of view—namely, with respect to our proper reference frame S'—we observe them as if they were located at point B', associated with a curvature radius of $R - D$.

This situation becomes analogous to the accelerating rod (Fig. 14). In that scenario, we observed that time advanced more rapidly at the front end A of the rod, a result we expressed in terms of frequencies in Eq. (26). Applied to a cosmological scale, the same phenomenon implies that light emitted (ω_B) by nearby celestial bodies with low recession velocities will invariably be received with a redshift (ω_A). Hence, within this harmonic model of the universe, the nearby naturally appears to be expanding.

If we rearrange Eq. (26) in terms of the redshift z and the rod's length L' is replaced by the distance D separating us from the clusters B and C, we obtain:

$$1 - \frac{D}{R} = \frac{\omega_A}{\omega_B} \quad \Rightarrow \quad z \equiv \frac{\omega_B - \omega_A}{\omega_A} = \frac{D/R}{1 - D/R} = \frac{\omega_B}{\omega_A} \cdot \frac{D}{R}, \tag{55}$$

For small values of redshift ($z \ll 1$ or $\omega_B \approx \omega_A$), Hubble's law is recovered. Conversely, for values $z \gg 1$, the redshift initially remains similar to the value predicted by the standard model as can be seen in Fig. 27. However, as we approach distance values

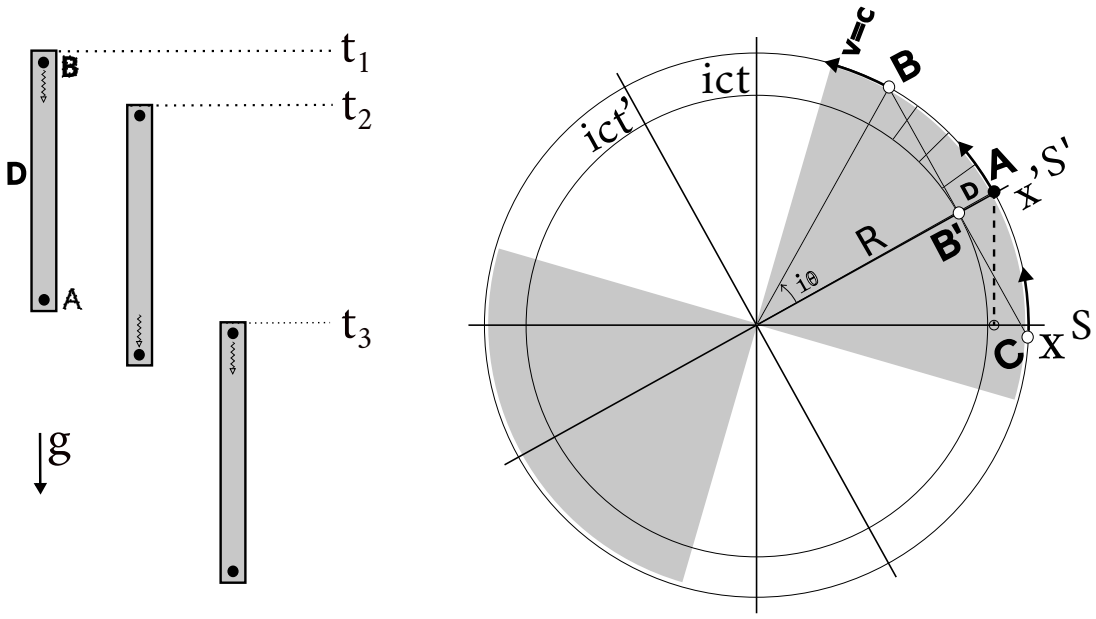

Fig. 26 Left: Depicts three different instants of a rod of proper length D accelerating under the effect of a gravitational field (free fall). The front end A acts as a receiver of the signals sent by the rear end B, which are emitted at a proper frequency ω_B and received at A at ω_A. **Right:** This same situation is shown in circular representation. As the rod falls, it increases its velocity with respect to the fixed axes S. The rear end B' runs on the inner circle of radius $R - D$, and the front end on the outer one of radius R. This situation also corresponds to that of two galaxy clusters A and B rotating in the universe's spacetime wheel according to the fundamental cosmic cycle. The distance D is the distance at which a body must be located to exhibit a recession velocity equal to v_g. However, it can also be understood as the apparent reduction in the radius of curvature of the galaxy cluster located at point B (or C), as perceived by an observer at point A. That is, the distant cluster at B appears to revolve in spacetime with an effective radius of curvature given by $R_B = R - D$. The ratio between the frequencies of the signals emitted by B (or C) and those received at A is given by Eq. (55).

D comparable to the curvature radius R—that is, for recession velocities of the order of c—the values diverge from the ΛCDM model prediction [31, 32]. This discrepancy is understandable, since Eq. (55) does not account for the background cycle of the universe. To clarify, it is as if, in the example of the two bodies in free fall through a tunnel bored through the Earth, we had assumed that they always maintain the same distance D relative to each other. While this may seem plausible from the perspective of A, it is evident from an external viewpoint that the situation is quite different—and it likely influences the final outcome in one way or another.

By comparing Eq. (55) with the Hubble–Lemaître law, $z = (H_0 D)/c$, we can derive an expression for the Hubble constant:

$$H_0 = \frac{c\,\omega_B}{R\,\omega_A} \approx \frac{c}{R}, \tag{56}$$

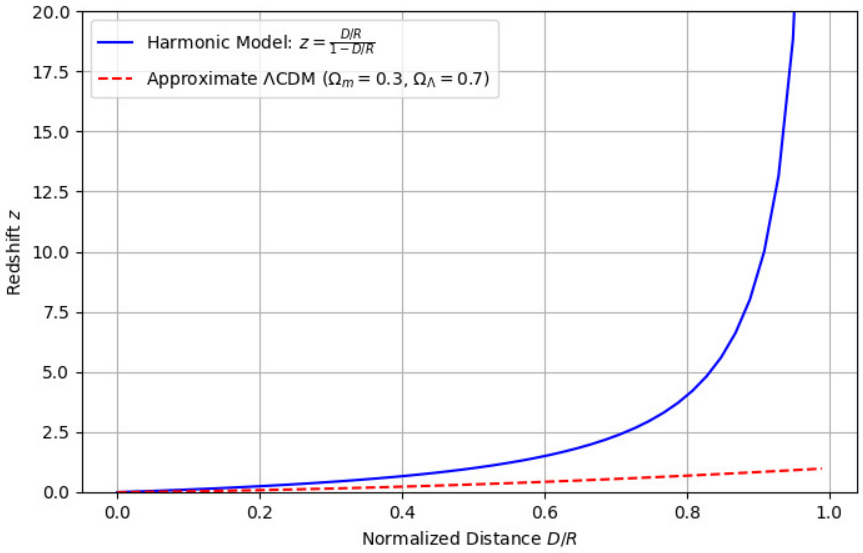

Fig. 27 Graphical comparison between the redshift obtained from the harmonic model, where the received frequency ω_A is related to the emitted frequency ω_B through $\omega_A = \omega_B(1 - D/R)$, and the redshift predicted by the standard cosmological model (ΛCDM, with typical parameters $\Omega_m = 0.3$ and $\Omega_\Lambda = 0.7$) [33].

where the approximation holds in the limit of small redshift ($\omega_A \approx \omega_B$), which is precisely the regime where Hubble's law remains valid.

As mentioned above, the fact that θ remains constant implies that subsequent measurements of v_g yield the same result. Similarly, D and a_g remain unchanged—unless the rotation of both A and B in spacetime relative to the fixed axes of the flat spacetime frame S (in Fig. 24) modifies these values over time. Therefore, within this model, the accelerating expansion has a somewhat illusory character, akin not to an optical illusion, but rather to one arising from gravitational time dilation, which distorts the perception of motion over cosmological distances.

Finally, it is worth noting that the right-hand side of Eq. (56) corresponds to the angular frequency of the universe's rotation in spacetime. Therefore, if the value of the Hubble constant is known, it is possible to derive the universe's lifespan from it. According to the measurement by Riess et al. [34], based on a Cepheid–Type Ia supernovae sample, the Hubble constant is $H_0 = 73.01 \pm 0.99 \mathrm{km/(s \cdot Mpc)}$. From this, the universe's lifespan T is obtained as:

$$T = \frac{1}{2}\left(\frac{2\pi}{H_0}\right) = (4.22 \pm 0.06) \times 10^{10}\,\mathrm{yr} \approx 42.2 \quad \text{billion years}, \tag{57}$$

where the division by 2 accounts for the fact that the cosmological cycle is completed twice in one full 2π rotation (see Fig. 28).

Alternatively, if one uses the value of the Hubble constant inferred from early-universe observations of the cosmic microwave background by the ESA *Planck* mission under the assumption of a flat ΛCDM model [32, 35], namely $H_0 = 67.66 \pm 0.42$ $(km/s)/Mpc$, the lifespan derived from Eq. (57) changes to $T \approx 45.5$ billion years.

6.2 Reinterpreting Dark Matter

Let us now return to the original interpretation of the *fundamental cycle*, not as a rotation in spacetime but rather as an alternation between *presence* and *absence* (Fig. 28).

It is noteworthy that, regardless of the extent of *presence* in the universe, the cycle consistently follows the same curvature. This implies that the corresponding gravitational value, given by $g = c^2/R$, remains constant even as *presence* (i.e., space) diminishes in favor of *absence* (i.e., time). In other words, *absence* also contributes gravitationally.

In this sense, absence can be connected to dark matter, as both are invisible yet exert a gravitational influence [36]. At this point, one might argue that *dark energy* should also be included in this category; however, it is a hypothetical form of energy introduced to explain the universe's accelerating expansion—a phenomenon that, within the present framework, emerges as an intrinsic feature. Therefore, invoking dark energy is not necessary in this context.

The current cold dark matter density of the universe is estimated to be $\Omega_c = 0.265$ [37], meaning that approximately 26.5% of the total energy content of the universe consists of dark matter. This value can be interpreted geometrically as shown in Fig. 28-*Left*, where the dark region represents 26.5% of a unit circle. Consequently, for a circle of unit area, one has $Y^2 = 0.265$. From this, the angle α corresponding to point (2) in Fig. 28-*Right*, which represents a hypothetical expansion phase of the universe, can be calculated as $\alpha = \cos^{-1}\sqrt{0.265} \approx 59.02°$. By relating this angle to the current age of the universe, again it becomes possible to estimate the full duration of a cosmological cycle—that is, the time between two successive Big Bang events.

In Fig. 28-*Right*, the angle between two consecutive Big Bangs (represented as two black circles) is 180°. Dividing this value by the angle just obtained yields $180°/59.02° \approx 3.05$, which corresponds to the factor by which the current age of the universe must be multiplied to obtain its total lifespan. Given that the present age of the universe is estimated at 13.787 ± 0.020 billion years [32], this leads to the following approximation for the full duration of the universe's period:

$$T \approx 3.05 \times 13.787 \approx 42.07 \text{ billion years.} \tag{58}$$

which is consistent with Eq. (57).

Once the period T of the cosmological cycle is determined, the corresponding angular frequency ω can be calculated. Since the cycle is completed twice during a full 2π rotation, the angular frequency is given by $\omega = 2\pi/(2T) \approx 2.369 \times 10^{-18}$ rad/s. Having determined the angular frequency, one can then infer the spacetime radius of

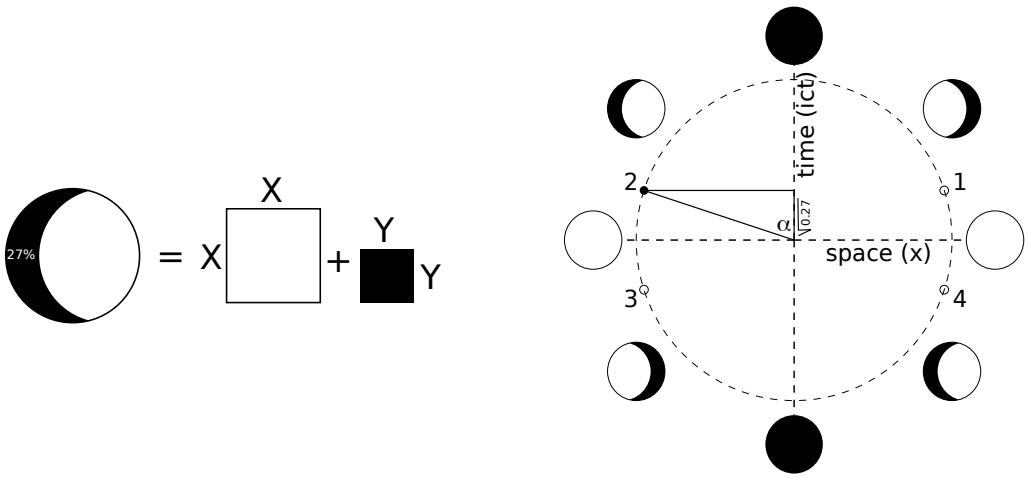

Fig. 28 Left: The amount of dark matter in the universe is currently estimated at $\Omega_c \approx 0.265$. **Right:** Representation of the universe's cycle as a UCM that transforms presence (space) into absence (time), and vice versa—or equivalently, ordinary matter into its dark counterpart. All points labeled (1) through (4) correspond to the same amount of dark matter. However, while points (2) and (4) lie in an expansive phase of the universe, points (1) and (3) correspond to contraction phases. The currently observed amount of dark matter determines the vertical leg of the triangle, which equals $\sqrt{0.265}$. Assuming the universe is in an expanding state—as in either (2) or (4)—the angle is $\alpha \approx 59.02°$, which, combined with the current age of the universe, determines its overall lifespan.

the universe and its associated curvature κ. The radius R follows from the definition $R = c/\omega \approx 1.27 \times 10^{26}$ m, which yields a corresponding curvature of $\kappa = R^{-1} \approx 7.9 \times 10^{-27}\ m^{-1}$. According to this model, this would correspond to a non-zero value of spacetime curvature, differing by at least one order of magnitude from the estimate derived within the FLRW metric, given by $\kappa \approx \left(H_0\sqrt{|\Omega_k|}\right)/c \approx 2.5 \cdot 10^{-28}$ m^{-1}, assuming $H_0 \approx 73$ km·s^{-1}·Mpc^{-1} and $\Omega_k = 0.001$ [38].

6.3 Our Phase in the Cycle of the Universe

According to the proposed correspondence between *absence* and dark matter, determining our current phase within the cosmological cycle amounts to examining how the observed quantity of dark matter evolves over time. A decreasing value would indicate an expanding phase of space, whereas an increasing value would suggest a contracting phase.

In this context, the agreement between the two independent estimations of the universe's lifespan—given by Eqs. (58) and (57)—supports the interpretation that we are currently in an expansive phase. Specifically, the fact that both lifespan values coincide implies that, from our vantage point, the universe is evolving toward a state of maximum expansion, corresponding to points (2) and (4) in Fig. 28.

Conversely, had we assumed that we are in a contracting phase of space—represented by points (1) and (3) in Fig. 28—then, for the same observed dark matter fraction of 26.5%, the corresponding angle would have been $\alpha = 180° - 59.02° =$

120.98°, leading to an estimated universe period of $T \approx 20.5$ billion years, which no longer aligns with the estimate provided in Eq. (57). This discrepancy reinforces the view that we are currently situated in an expansive stage of the cosmic cycle.

6.4 A Universe Relative to the Observer

The cosmic cycle, manifested through the growth and decay of dark matter, simultaneously governs the expansion and contraction of spatial perception. In this framework, the phase corresponding to a universe devoid of space aligns with what physics refers to as the initial instant or Big Bang, which, due to the cyclical nature of the model, coincides with the final instant or Big Crunch.

However, our approach introduces a fundamental departure from the conventional notions of the Big Bang or Big Crunch: whereas these concepts are usually associated with an absolute notion of space and time—implying that the universe begins or ends at a definite moment and location—in our model, such events are treated as phases relative to the observer. Indeed, according to the fundamental cycle, every physical entity undergoes continuous rotation in spacetime relative to fixed axes, which represent flat spacetime. Each physical system evolves, at its own pace, through the phases symbolically represented by the moon-like stages in Fig. 29.

As depicted in the figure, while point A is approaching a phase of maximum spatial expansion (represented by a white circle), points B and C have already entered a phase of contraction. This implies that, within the present model, the Big Bang—or any other cosmological stage—is relative to the observer, in the sense that it does not occur simultaneously for all regions of the universe. Rather, it depends on the observer's specific position along the wheel of spacetime. Fortunately, there is a familiar analogy that perfectly illustrates this concept: the daily cycle of day and night on Earth. *Just as some time zone on Earth is currently witnessing sunrise, there exist regions in the universe that are now undergoing their own Big Bang.*

6.5 A Brief Note on Entropy

An important consideration regarding the cyclic nature of the proposed model is the treatment of entropy. While Einstein once envisioned a universe that expands and contracts eternally [39], Tolman argued that such a scenario would be difficult to reconcile with the second law of thermodynamics [20]. This issue has since been revisited in various modern cyclic cosmologies. For instance, Steinhardt and Turok [40–42] introduced dark energy and brane collisions to address entropy growth, while Baum and Frampton [43, 44] explored the implications of phantom energy. Other approaches, such as Penrose's conformal cyclic cosmology (CCC) [45, 46] and loop quantum cosmology [47], propose distinct mechanisms to reset or absorb entropy, including black hole evaporation and quantum degrees of freedom.

In contrast, the framework presented here naturally gives rise to four distinct temporal regimes (see Fig. 29), where time may take on positive or negative values, and may either increase or decrease. This richer structure of time within each cycle could offer a novel perspective on the entropy problem, suggesting that conventional

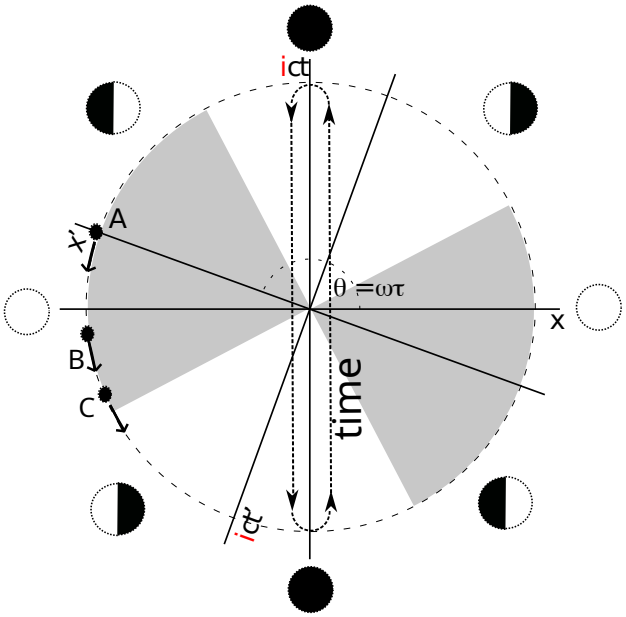

Fig. 29 Illustrates the fixed axes of the universe (reference system S), which represent flat spacetime, along with our hypothetical location (A) within the universe's cycle and our proper reference frame S'. In the configuration suggested by the results of the previous section, we would be approaching a point of maximum expansion, whereas points B and C, representing distant galaxy clusters, would already perceive a contracting universe since the moment of maximum expansion has already occurred for them. The figure also explicitly portrays the temporal cycle progressing along the y-axis, thereby emphasizing that the treatment of entropy within this model enters a novel framework.

thermodynamic reasoning might require reformulation in such a context. A detailed analysis of these implications is left for future work.

7 Conclusions

To avoid spontaneous generation, it was first assumed that the universe follows a cycle—named as the fundamental cycle—where two different "substances", presence and absence, alternate with each other. To account for their antagonistic natures, the imaginary unit i was introduced representing the inconceivability of the absence when experienced from the presence. Such a point of view was referred to as a "view from inside" because it considered the fact that we belong to the structure. Representing this cycle in terms of a uniform circular motion, an expression similar to the relativistic invariant interval was found. The latter allowed us to physically interpret the presence in terms of space and the absence in terms of time. At this point, the fundamental cycle became a spacetime rotation, and the corresponding coordinate transformation—achieved by an axis rotation—manifested as the Minkowski rotation, which is formally equivalent to the Lorentz transformation.

Therefore, relativity appears to be consistent with the idea of a universe composed of two antagonistic natures that alternate cyclically, and with the fact that, from

our perspective—being embedded within the structure—one of them appears to us as inconceivable. While cyclicity is taken into account by the rotation, this inherent inconceivability is represented by the imaginary unit.

Thus, the imaginary nature of time, first introduced by Poincaré (1906) [2] in the form ict, acquires a concrete physical interpretation: it reflects the inconceivability of absence—or a "beyond"—that emerges as soon as the observer is included as part of the physical system. In this context, the Wick rotation, considered here as $y \to iy$, is interpreted as a transformation that shifts the perspective from an external to an internal frame of reference within the system.

This shift in perspective also entails profound algebraic consequences. Specifically, the introduction of the imaginary unit into the axes rotation transformation breaks the correspondence between the geometric representation of various quantities and their respective algebraic values. Nevertheless, we have observed that the underlying relational structure among those quantities remains intact—except for the time reversal effect.

Specifically, we found that the cosine and sine of an imaginary angle can still be used to project onto the plane, even though the algebraic values of these projections no longer coincide with their geometric interpretation. This proved to be a powerful analytical tool, primarily because it enables the geometric derivation of key relativistic phenomena. In other words, circular geometry can effectively be employed as a conceptual framework for understanding relativity. This realization, together with the dynamism of the fundamental cycle, ultimately led us to the harmonic interpretation of relativity.

Indeed, the harmonic interpretation of relativity arises from the UCM characteristic of the fundamental cycle, combined with the possibility of projecting it onto the axes using the cosine and sine functions of an imaginary angle. Within this interpretation, a particle in an inertial state is understood as a particle that follows its own fundamental cycle, which consists of a spacetime rotation with linear velocity equal to the speed of light c and radius R equal to the curvature radius.

In particular, when this spacetime rotation is projected onto the real (spatial) axis, it results in a form of complex Simple Harmonic Motion (SHM*) with proper velocity v_τ and proper acceleration a_τ. In this context, the product of v_τ and the rest mass m_o corresponds to the relativistic momentum, while the product of $m_o R$ and a_τ yields the relativistic energy.

This interpretation allows the rest energy to be understood as analogous to the elastic potential energy of a spring at its maximum elongation—geometrically speaking. In contrast, relativistic momentum arises only in phases other than maximum elongation and is associated with the contraction or expansion velocity of the spring. Since we are centered on our own reference axes, we always perceive ourselves as being at rest—i.e., at the point of maximum elongation. Other bodies, however, which also undergo rotation in spacetime but exhibit a certain phase lag relative to us, are perceived from our reference frame as occupying a different point in the spring's oscillation. Consequently, they are associated with a radial velocity, which is what gives rise to their recession momentum relative to us.

Furthermore, we interpreted the acceleration a_τ as a manifestation of gravity. Since gravity also emerges naturally from the fundamental cycle, this framework provides a unified setting in which both the laws of special relativity and the essential ingredient of GR—gravity—coexist coherently.

Moreover, within this harmonic reinterpretation of relativity, two novel expressions—namely, Eqs. (41)–(42)—have emerged, potentially offering a new perspective on relativistic dynamics.

We have also seen that the core of the relativistic Lagrangian for a free particle still takes the form $T - V$, where V represents the relativistic energy and indeed resembles an elastic potential energy. We have observed that the resulting complex harmonic behavior is characterized by an elastic constant k, and we have raised—but not resolved—the question of whether this constant might be related to the cosmological constant.

Perhaps most surprisingly, we found that the relativistic harmonic cycle, or fundamental cycle, comprises eight distinct phases, in contrast to the familiar four-phase expansion-contraction cycle of the classical simple harmonic oscillator. Of these eight phases, only four are directly observable, and among those, only two correspond to positive energy states. The remaining two exhibit negative energy and evolve with time reversed. We have therefore interpreted this domain as corresponding to antimatter. The other unobservable half unfolds in a regime where relative velocities v_g exceed the speed of light. Particles inhabiting this beyond are characterized by imaginary values of position, momentum, and energy. Yet, despite their imaginary and therefore inconceivable or unobservable nature, we have argued that this realm borders our real world and thus must produce some kind of real manifestation. In other words, although it cannot be accessed or perceived from within, we may nonetheless be observing its outer boundary.

Since this shift in perspective—from inside to outside or vice versa—is precisely the physical meaning of the Wick rotation, it compelled us to multiply once again by the imaginary unit. While the first rotation led us from the external to the internal domain, this second one brought us from the internal to the external, now accompanied by the negative sign that follows from the operation $i \cdot i = -1$, which we interpreted, by geometric equivalence, as a rotation of $180°$. This reasoning enabled us to associate an external and real manifestation with the imaginary realm, such that the fundamental cycle is ultimately expressed in eight distinct phases, each one manifesting itself in some way to the observer.

Subsequently, we quantified all possible relativistic situations between the object and the subject, yielding a total of $8 \cdot 8 = 64$. At this point, we noted that this structure—eight distinct stages and their 64 relativistic configurations—bears a striking parallel to the cosmology of ancient China. In this regard, it would be particularly interesting, especially from an interpretative perspective, to investigate whether this correspondence has any solid foundation.

Another particularly interesting feature of the fundamental cycle is that it is not exclusive to the universe as a whole but must be present at all scales, in the same way that the laws of relativity apply universally. This implies that such a cycle of spacetime mesh transformation must also occur at the level of fundamental particles.

Since this domain is governed by high-frequency cycles, our analysis suggests that the curvature radii associated with the fundamental cycle of these particles could be extremely small.[13] This idea aligns with other theoretical contexts such as string theory, loop quantum gravity, or models of anti-gravitating charge [48–50]. There also exist well-known physical phenomena that may be directly related to it, such as Dirac's *Zitterbewegung* [51, 52] or neutrino oscillations [53].

It is also worth noting that the requirement for the time variable and the imaginary unit to always appear together—confirmed by the present macroscopic-scale analysis—is consistent with the quantum mechanical principle $\langle\Phi|\Psi\rangle = \langle\Psi|\Phi\rangle^*$, which implies that changing the sign of the imaginary unit i is equivalent to reversing the direction of time.

At the opposite end of the scale, when the fundamental cycle is considered at its largest possible extension, profound implications arise at the cosmological level. To begin with, it gives rise to a cyclic model of the Universe in which time gradually transforms into space, and space into time. A more detailed analysis further reveals that half of our observable cosmological domain—that corresponding to $v_g < c$ and positive energies—must be characterized by accelerated expansion, an outcome that is consistent with current experimental observations.

In particular, the accelerated expansion considered here displays the peculiar property that consecutive measurements of a celestial body's recession velocity yield identical results, even though the body is undergoing acceleration. This apparent paradox finds an explanation in the phenomenon of gravitational time dilation. Therefore, it may be concluded that the effect of accelerated expansion is, to some extent, an observational illusion. Nevertheless, we have also noted that this scenario is superimposed on a dynamic, cyclic background governed by the universe's fundamental cycle, which may modulate the observed expansion. Indeed, assuming that the accelerated expansion scenario is a fixed one—fixed in the sense that consecutive measurements of distance and velocity associated with distant cosmic objects always yield the same values—is analogous to assuming that two objects in free fall through a tunnel crossing the Earth maintain a constant relative distance between them. That is, one must take into account that, although from our reference frame the scenario may appear to be static—since our relative angle θ with respect to these distant bodies does not change—we cannot overlook the fact that, in the background, the universe's cycle continues to unfold. This cycle causes space itself—and time—to undergo 8 different stages, and therefore must modulate our final perception in some way. Understanding the nature of this modulation would be of great interest.

We have also pointed out that, regardless of the amount of presence in the universe, the fundamental cycle between presence and absence always follows the same curvature. This implies that absence also interacts gravitationally and, therefore, has been identified with Zwicky's dark matter. This interpretation has made it possible to calculate the period of the universe by combining the current amount of dark matter with the present age of the universe, yielding a result of $T \approx 42.07$ billion years.

[13] We do not address this here, as the analysis requires a separate and dedicated article, but there are indications suggesting that the curvature radius associated with such microscopic particles could be on the order of their Compton wavelength.

A similar value ($T \approx 42.2 \pm 0.6$) for the universe's period has also been obtained through an alternative approach. In this case, the distance D—in Figs. 24 and 26—has been interpreted as the amount by which the curvature radius of the object is reduced from the observer's point of view. This reduction causes the observer to perceive the object as if it were under the influence of a stronger gravitational field and, consequently, gravitational time dilation leads this difference to manifest as a redshift. In this way, we have derived an expression for the Hubble–Lemaître law.

Specifically, for small redshift values, we have found that the Hubble constant directly corresponds to the rotational frequency associated with the universe's cycle. This has allowed us to recalculate its period, which—when using the value of H_0 obtained through "late universe" techniques—is in good agreement with the previously derived result. However, when using "early universe" techniques to determine the Hubble constant, the resulting period does not align as well with the independently derived value, thereby providing a first argument in favor of interpreting the Hubble tension as an indication that the late universe measurements may more accurately reflect the underlying cosmological dynamics.

As for the phase in which we currently find ourselves within the universe's cycle, the only conclusion we can draw at this point is that the agreement between the two computed values of the period suggests that, from our perspective, we are observing a phase in which space is evolving toward its point of maximum expansion (points 2 and 4 in Fig. 28).

Another significant aspect of this cosmological model is the abandonment of the notion of a Big Bang as a spatially centered event occurring at a single, universal initial moment for all regions of the universe. Instead, this event is reinterpreted as a phase within a larger cosmological cycle, experienced at different times depending on the observer's location within the cycle. To clarify this idea, we have drawn an analogy with the terrestrial day-night cycle: just as the sunrise occurs at different times in different locations on Earth, there are regions of the universe that, at this very moment, are undergoing their own Big Bang phase.

In summary, the universe model proposed by the fundamental cycle describes a cyclic cosmos whose dynamics should be observable through the increase or decrease of dark matter. It is an observer-dependent universe, and our current phase corresponds to a period in which the amount of dark matter is declining. In this framework, the scenario of accelerated expansion is interpreted as a fixed and partially illusory effect, superimposed on a deeper, cyclic background—the fundamental cycle of the universe—which may modulate our perception of cosmic expansion.

These findings open up interesting directions for future research. The idea of a harmonic reinterpretation of relativity leads to the possibility that the dynamical behaviour of spacetime, as described in GR, could emerge from a superposition of fundamental cycles. In this view, spacetime curvature and evolution might be reinterpreted as the collective effect of a spectrum of harmonic oscillators, each governed not by traditional real-valued Simple Harmonic Motion, but by its complex-valued counterpart.

Although the approach developed here provides strong support for the existence of a fundamental cycle as a unifying organizational principle in nature, operating coherently across all physical scales, it is important to note that at microscopic scales, the assumption of continuous time flow may no longer hold. Instead, a discrete temporal structure may need to be considered, as suggested by approaches such as loop quantum gravity [54]. Further work will be required to explore how this transition from continuous to discrete dynamics might be incorporated into the present framework.

Note

The original manuscript was written in Catalan. Some portions of the English translation were assisted using AI-based language tools (ChatGPT), under the author's full supervision.

References

[1] Minkowski, H.: Raum und Zeit. Physikalische Zeitschrift, Garden City, NY (1909). English translation in: Lorentz, H. A., Einstein, A., Minkowski, H., Weyl, H. (1952). *The Principle of Relativity*. Dover Publications.

[2] Poincaré, H.: Sur la dynamique de l'électron. Rendiconti del Circolo Matematico di Palermo **21**, 129–176 (1906) https://doi.org/10.1007/BF03013466

[3] Barrett, J.F.: The Hyperbolic Theory of Special Relativity. arXiv:1102.0462 [physics.gen-ph]. Version 2, revised 16 Sep 2019 (2011). https://doi.org/10.48550/arXiv.1102.0462

[4] Peskin, M.E., Schroeder, D.V.: An Introduction to Quantum Field Theory. Addison-Wesley, Reading, Massachusetts (1995)

[5] Weinberg, S.: The Quantum Theory of Fields. Vol. 1: Foundations. Cambridge University Press, Cambridge, UK (1995)

[6] DeWitt, B.S.: Quantum theory of gravity. i. the canonical theory. Physical Review **160**(5), 1113 (1967) https://doi.org/10.1103/PhysRev.160.1113

[7] Hartle, J.B., Hawking, S.W.: Wave function of the universe. Physical Review D **28**(12), 2960–2975 (1983) https://doi.org/10.1103/PhysRevD.28.2960

[8] Hawking, S.W.: The quantum state of the universe. Nuclear Physics B **239**(1), 257–276 (1984) https://doi.org/10.1016/0550-3213(84)90093-2

[9] Aharonov, Y., Vaidman, L.: Properties of a quantum system during the time interval between two measurements. Physical Review A **41**, 11–20 (1990) https://doi.org/10.1103/PhysRevA.41.11

[10] Witten, E.: On holomorphic factorization of wzw and coset models. Communications in Mathematical Physics **144**(1), 189–212 (1991) https://doi.org/10.1007/BF02099116

[11] Isham, C.J.: Canonical quantum gravity and the problem of time. arXiv preprint gr-qc/9210011 (1992)

[12] Barbour, J.B.: Time and complex numbers in canonical quantum gravity. Physical Review D **47**(12), 5422–5429 (1993) https://doi.org/10.1103/PhysRevD.47.5422

[13] Hooft, G.: Quantum mechanics and determinism. arXiv preprint hep-th/0105105 (2001)

[14] Penrose, R.: The Road to Reality: A Complete Guide to the Laws of the Universe. Jonathan Cape, London (2004)

[15] Aharonov, Y., Rohrlich, D.: Quantum Paradoxes: Quantum Theory for the Perplexed. Wiley-VCH, Weinheim, Germany (2005)

[16] Smolin, L.: The Trouble With Physics: The Rise of String Theory, The Fall of a Science, and What Comes Next. Houghton Mifflin, Boston (2006)

[17] Popov, V.S.: Imaginary-time method in quantum mechanics and field theory. Physics of Atomic Nuclei **68**(4), 686–708 (2005) https://doi.org/10.1134/1.1903097

[18] Huang, Y.-C.: A route toward quantum gravity through the imaginary-time field theory. arXiv preprint **arXiv:1312.4380** (2013)

[19] Wick, G.-C.: Properties of bethe-salpeter wave functions. Physical Review **96**(4), 1124 (1954) https://doi.org/10.1103/PhysRev.96.1124

[20] Tolman, R.C.: Relativity, Thermodynamics, and Cosmology. Oxford University Press, Oxford (1934)

[21] Steinhardt, P.J., Turok, N.: A cyclic model of the universe. Science **296**(5572), 1436–1439 (2002) https://doi.org/10.1126/science.1070462

[22] Penrose, R.: Cycles of Time: An Extraordinary New View of the Universe. Bodley Head, London (2010)

[23] Recami, E., Mignani, R.: Classical theory of tachyons (special relativity extended to superluminal frames and objects). Rivista del Nuovo Cimento (1971-1977) **4**(2), 209–290 (1974)

[24] Recami, E.: Tachyons, monopoles, and related topics. North-Holland (1986)

[25] Székely, G.: On the logical consistency of the existence of faster-than-light

particles. European Journal of Physics **41**(3), 035601 (2020)

[26] Ehrlich, R.: Evidence for tachyons. Astroparticle Physics **66**, 11–17 (2015)

[27] Feynman, R.P.: The theory of positrons. Physical Review **76**(6), 749–759 (1949) https://doi.org/10.1103/PhysRev.76.749

[28] Goldstein, H.: Classical Mechanics, 2nd edn. Addison-Wesley, Reading, Massachusetts (1980)

[29] Haramein, N., Rauscher, E.A.: The origin of spin: A consideration of torque and coriolis forces in einstein's field equations and grand unification theory. In: Amoroso, R.L., Lehnert, B., Vigier, J.-P. (eds.) Beyond the Standard Model: Searching for Unity in Physics, pp. 153–168. The Noetic Press, Oakland, CA (2005)

[30] Hubble, E.: A relation between distance and radial velocity among extra-galactic nebulae. Proceedings of the National Academy of Sciences of the United States of America **15**(3), 168–173 (1929) https://doi.org/10.1073/pnas.15.3.168

[31] Efstathiou, G., Sutherland, W.J., Maddox, S.J.: The cosmological constant and cold dark matter. Nature **348**, 705–707 (1990) https://doi.org/10.1038/348705a0

[32] Riess, A., *et al.*: Planck 2018 results. vi. cosmological parameters. Astronomy & Astrophysics **641**, 6 (2020)

[33] Perlmutter, S., *et al.*: The supernova cosmology project. The Astrophysical Journal **517**, 565–586 (1999)

[34] Riess, A., *et al.*: Cluster cepheids with high precision gaia parallaxes, low zero-point uncertainties, and hubble space telescope photometry. The Astrophysical Journal **938**, 36 (2022)

[35] Cruz, M., Anderson, R.: A 0.9% calibration of the galactic cepheid luminosity scale based on gaia dr3 data of open clusters and cepheids. Astronomy & Astrophysics **672**, 85 (2023)

[36] Zwicky, F.: Die rotverschiebung von extragalaktischen nebeln. Helvetica physica acta **6**, 110–127 (1933)

[37] Tanabashi, M., (Particle Data Group).: Astrophysical constants and parameters. Physical Review D. **98 (3)**, 030001 (2019)

[38] Ryden, B.: Introduction to Cosmology, 2nd edn., pp. 142–145. Cambridge University Press, Cambridge, UK (2017). Chap. 6

[39] Einstein, A.: Zum kosmologischen problem der allgemeinen relativitätstheorie. Sitzungs. König. Preuss. Akad., 235–237 (1931)

[40] P. J. Steinhardt, N.T.: A cyclic model of the universe. Science. **296 (5572)**, 1436–1439 (2001)

[41] P. J. Steinhardt, N.T.: Cosmic evolution in a cyclic universe. Physical Review D. **65 (12)**, 126003 (2002)

[42] P. J. Steinhardt, N.T.: The cyclic model simplified. New Astronomy Reviews **49 (2–6)**, 43–57 (2005)

[43] L. Baum, P.H.F.: Entropy of contracting universe in cyclic cosmology. Modern Physics Letters A **23 (1)**, 33–36 (2008)

[44] L. Baum, P.H.F.: Turnaround in cyclic cosmology. Physical Review Letters **98 (7)**, 071301 (2007)

[45] Penrose, R.: Before the big bang: An outrageous new perspective and its implications for particle physics. Proceedings of the EPAC, Edinburgh, Scotland:, 2759–2762 (2006)

[46] Penrose, R., Gurzadyan, V.G.: On ccc-predicted concentric low-variance circles in the cmb sky. Eur. Phys. J. Plus. **128 (2)**, 22 (2013)

[47] A. Ashtekar, E.B.: A short review of loop quantum gravity. Rep. Prog. Phys. **84**, 042001 (2021)

[48] Zwiebach, B.: A First Course in String Theory, 1st edn. Cambridge University Press, Cambridge, UK (2004)

[49] Rovelli, C.: Quantum Gravity. Cambridge University Press, Cambridge, UK (2004)

[50] Burinskii, A.: The dirac-kerr electron. Gravitation and Cosmology **14**, 109–122 (2008) https://doi.org/10.1134/S0202289308020031

[51] Dirac, P.A.M.: The quantum theory of the electron. Proceedings of the Royal Society A **117**(778), 610–624 (1928) https://doi.org/10.1098/rspa.1928.0023

[52] Schliemann, J., Loss, D.: Zitterbewegung of electrons in semiconductors. Physical Review B **71**(8), 085308 (2005) https://doi.org/10.1103/PhysRevB.71.085308

[53] Kajita, T.: Nobel lecture: Discovery of atmospheric neutrino oscillations. Reviews of Modern Physics **88**(3), 030501 (2016) https://doi.org/10.1103/RevModPhys.88.030501

[54] Abhay Ashtekar, T.P., Singh, P.: Quantum nature of the big bang: An analytical and numerical investigation. Physical Review D **73**(12), 124038 (2006) https://doi.org/10.1103/PhysRevD.73.124038